Applied Geochemistry 26 (2011) 1649–1664

Contents lists available at ScienceDirect

Applied Geochemistry

journal homepage: www.elsevier.com/locate/apgeochem

Metal binding to dissolved organic matter and adsorption to ferrihydrite in shallow peat groundwaters: Application to diamond exploration in the James Bay Lowlands, Canada

Jamil A. Sader [a,*], Keiko Hattori [a], Stewart Hamilton [b], Kerstin Brauneder [a]

[a] University of Ottawa, Earth Sciences Department, Ottawa, Ontario, Canada K1N 6N5
[b] Sedimentary Geoscience Division, Ontario Geological Survey, Sudbury, Ontario, Canada P3E 2G9

ARTICLE INFO

Article history:
Received 30 September 2010
Accepted 21 April 2011
Available online 29 April 2011
Editorial handling by C. Reimann

ABSTRACT

The speciation and solubility of kimberlite pathfinder metals (Ni, Nd, Ba and K) in shallow peat groundwaters is investigated over the Yankee, Zulu and Golf kimberlites in the Attawapiskat region, James Bay Lowlands, Canada. The purpose of this study is to examine the relationship between dissolved organic matter (DOM) complexation with kimberlite pathfinder metals and determine the spatial distribution of those metals in shallow peat groundwaters along sampling transects over subcropping kimberlites. Nickel, Nd, Ba and K complexation with DOM and the adsorption of these metals onto ferrihydrite were calculated using Visual MINTEQ 3.0 and the NICA-Donnan database. Calculations predict almost 100% of soluble Nd, Ni and Ba form complexes with DOM at sampling sites with little to no contribution from upwelling groundwater (i.e., dissolved organic C (DOC) concentrations = 40–132 mg/L, pH = 3.9–5.5, and log ionic strength $\leqslant -3$). In only the most ombrotrophic peat groundwater conditions does a majority fraction of K bind to DOM. By contrast, under conditions with large contributions from upwelling groundwaters (i.e., DOC concentrations $\leqslant$40 mg/L, pH = 5.5–6.5, and log ionic strength = -3 to -2), as little as 10% of Nd and Ni, and 0% K and Ba are predicted to complex with DOM. The modeling calculations suggest the dominant control on metal–DOM complexation, particularly with respect to Ni and Nd, is competitive effects for DOM binding sites due to elevated ionic strength where there is evidence of strong groundwater upwelling. Visual MINTEQ modeling of metal adsorption on ferrihydrite surfaces predicts that under strong upwelling conditions, Ni and Nd are scavenged from solution due to increased ferrihydrite precipitation and decreased fractions of metals complexed with DOM. Analytical geochemical data are consistent with model predictions of metal adsorption on ferrihydrite. Total dissolved Ni and Nd concentrations at sites of strong upwelling are up to five times lower than waters with little to no upwelling and log ferrihydrite saturation indices ($\log SI_{ferr}$) indicate precipitation (values up to 5) at sites of strong groundwater upwelling. Where the majority of Ni and Nd complex with DOM and ferrihydrite is highly under saturated ($\log SI_{ferr} = -18$ to -5), the concentrations of total Ni and Nd are elevated compared to other sites along sampling transects. Metal complexation with DOM effectively inhibits metal scavenging from solution via adsorption and/or from forming secondary mineral precipitates. Also, because alkaline earth metals do not compete strongly with Ni and Nd for adsorption sites on ferrihydrite surfaces, but do compete strongly for insoluble organic sites, Ni and Nd are more likely to adsorb onto ferrihydrite.

© 2011 Elsevier Ltd. All rights reserved.

1. Introduction

Dissolved organic matter (DOM) in natural waters can strongly affect metal speciation. In biological applications, metal DOM complexes have the ability to render potentially harmful dissolved metals non-toxic, as these complexes are typically bio-unavailable to organisms (Bell et al., 2002; Bruland et al., 1991; Paquin et al., 2002; Perdue and Ritchie, 2005). Metal–DOM complexes can also prevent metal scavenging due to formation of secondary mineral precipitates or adsorption to insoluble substances (Cornell and Schwertmann, 1979, 2003; Hoch et al., 2000; Ravichandran et al., 1999; Tipping, 2002), and is best exemplified in wetland environments, where dissolved organic C (DOC) is a major component of the dissolved ions in peat groundwaters.

In mineral exploration, the ability of mobile ions to adsorb or precipitate onto mineral soil in the shallow subsurface (Cameron et al., 2004; Hattori et al., 2009; Mann et al., 1998; McClenaghan et al., 2006; Sader et al., 2009) or peat (Hattori and Hamilton, 2008) is effectively used to detect buried mineral deposits. Determining factors related to metal solubility such as pH and Eh are important when using water as an exploration tool to locate blind

* Corresponding author. Tel.: +1 613 614 2126; fax: +1 613 599 4904.
E-mail address: jamilsader@yahoo.com (J.A. Sader).

0883-2927/$ - see front matter © 2011 Elsevier Ltd. All rights reserved.
doi:10.1016/j.apgeochem.2011.04.022

mineral deposits (Leybourne and Cameron, 2010). However, most hydrogeochemical studies related to mineral exploration have not accounted for DOM influences on metal solubilities because the majority of natural groundwaters have low DOM concentrations. Additionally, soils for geochemical exploration are typically collected from locations that are above the water table. However, in environments with high concentrations of organic material, DOC is an integral part of metal solubility (Johannesson et al., 2004; Tipping, 2002) and may significantly impact the behaviour of potential ore deposit pathfinder metals in the shallow subsurface.

A previous geochemical study of peat groundwaters along sampling transects over Attawapiskat kimberlites identified elevated concentrations of Ni, Cr, light rare earth metals (LREEs), Ba, Rb and Cs, and high Ca/Mg ratios indicative of the presence of buried kimberlite (Sader et al., 2011). This study demonstrated pathfinder metals in peat groundwaters were primarily due to upwelling of deep groundwaters that had interacted with kimberlites. Metal concentrations well above baseline values were reported to extend up to 200 m beyond the kimberlite margins. The authors noted that Ni, Cr, LREEs and Ba are generally elevated at sites at or near kimberlite margins, where there is only small contributions from upwelling groundwater. Along sampling transects, high Ba, Rb and Cs concentrations were commonly observed at locations different from those with high Ni, Cr, and LREEs. The ratios of Mg/Ca were high at sites where transition, alkaline earth, and alkali pathfinder metals were also high compared to baseline values.

Herein the influence that high DOC contents in peat groundwaters may exert on pathfinder metal solubilities along sampling transects over subcropping kimberlites in the Attawapiskat kimberlite field, James Bay Lowlands, Canada, are examined. Peat groundwater metal concentrations and model calculations for metal speciation and the adsorption of soluble ions on ferrihydrite surfaces are presented. The interrelationship between metal–DOM complexes, and adsorption to ferrihydrite as a potential major sink for dissolved metals associated with buried kimberlite are explored. The goals of this paper are to: (1) identify the dominant controls related to variable metal–DOM complexation in peat groundwaters; (2) compare metal–DOM speciation calculations to analytical data; and (3) suggest possible mechanisms for scavenging metals from solution. The results of this study will likely be useful in the design and implementation of surficial geochemical exploration surveys in regions where soil and water organic content is high.

2. Location and geology

2.1. Geological setting, geology, and mineralogy of kimberlites

The kimberlites in this study are located in the James Bay Lowlands in north-central Canada, approximately 90 km west of the community of Attawapiskat, Ontario, and are within 15 km of DeBeers' Victor diamond mine (Fig. 1). The kimberlites intruded Paleozoic sedimentary rocks, predominantly composed of limestone, and underlying Archean igneous and metamorphic rocks in the mid-Jurassic (~170 Ma) (Norris, 1993; Webb et al., 2004) (Fig. 2). Host rock to the kimberlite at the bedrock surface is limestone of the Upper Attawapiskat Formation (Fig. 2), which locally crops out in the form of bioherms up to 2 m above the surrounding ground surface. Bioherms are reef cores composed of coral and skeletal remains of other marine organisms (Cowell, 1983). Kimberlites in this study form round to ellipsoid areal extents that range from 200 to 300 m in diameter (Fig. 3) and subcrop. Zulu kimberlite is the exception, as it crops out along its southern margin. A thin sheet of till (<1 m) and Tyrell Sea glaciomarine sediment

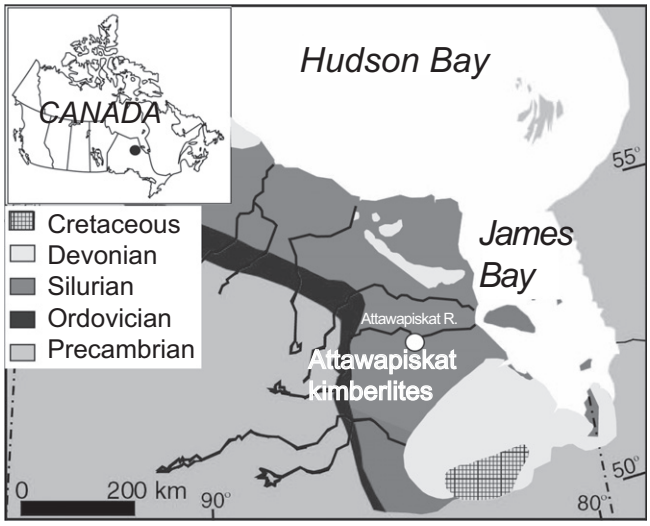

Fig. 1. Regional bedrock geology of the James Bay Lowlands and location of the Attawapiskat kimberlite field in north-central Canada (geological map modified from Bellefleur et al., 2005).

(2.1–21 m) (DeBeers, unpublished data) overlies the host Upper Attawapiskat Formation limestone and kimberlites in the study area (Fig. 2).

The region was glaciated during the Quaternary, during which time the bedrock surface was eroded and a thin till layer (<1 m) was deposited on the bedrock surface. Tyrell Sea sediment (TSS), comprised of fine-grained marine sand, silt and clay was deposited between 10 and 5 ka following the end of glaciation when the shoreline of James Bay (referred to as the Tyrell Sea during that period) extended inland approximately 300 km west and SW of its present location. Isostatic rebound resulted in ground surface elevation rises of 100–300 m since the retreat of the Laurentide ice sheet in the Attawapiskat region (Shilts, 1986). The present-day ground surface elevation is 80–90 m above sea level. Peat, approximately 2.5–3.4 m thick overlies the TSS and has been accumulating since the retreat of the Tyrell Sea approximately 5 ka BP. The peat is predominantly composed of sphagnum and is increasingly more humified with depth (i.e., the sphagnum is increasingly less recognizable below 0.5 m).

The Yankee kimberlite is located between outcropping bioherms SW and NE of the kimberlite (Fig. 3). The ground surface forms a gently sloping bowl-shape depression over the kimberlite that extends 150 m beyond its margin. The Zulu kimberlite is located east of a lobate raised bog and north of a small bioherm (Fig. 3). Ground surface at the Golf kimberlite is similar to that at Zulu, as both slope gently from west to east. No bioherms were observed near the Golf transect.

The mineralogy of the Attawapiskat kimberlites consists of abundant olivine macrocrysts, ilmenite, garnet, Cr-diopside, phlogopite and spinel (Armstrong et al., 2004; Kong et al., 1999; Sage, 2000). Kimberlite groundmass mainly consists of carbonate, spinel and serpentine with lesser monticellite, mica, apatite and perovskite (Kong et al., 1999). All kimberlites in the Attawapiskat field are either hypabyssal or volcaniclastic (Kong et al., 1999; van Straaten et al., 2009). Kimberlites sampled in this study (Yankee, Zulu, and Golf) are altered hypabyssal facies (Sage, 2000).

2.2. Peat groundwater hydrogeology and geochemical parameters

Hydrogeological measurements in the peat and TSS groundwaters of the Yankee and Zulu transects have been previously reported by Sader et al. (2011). To summarize, the water table

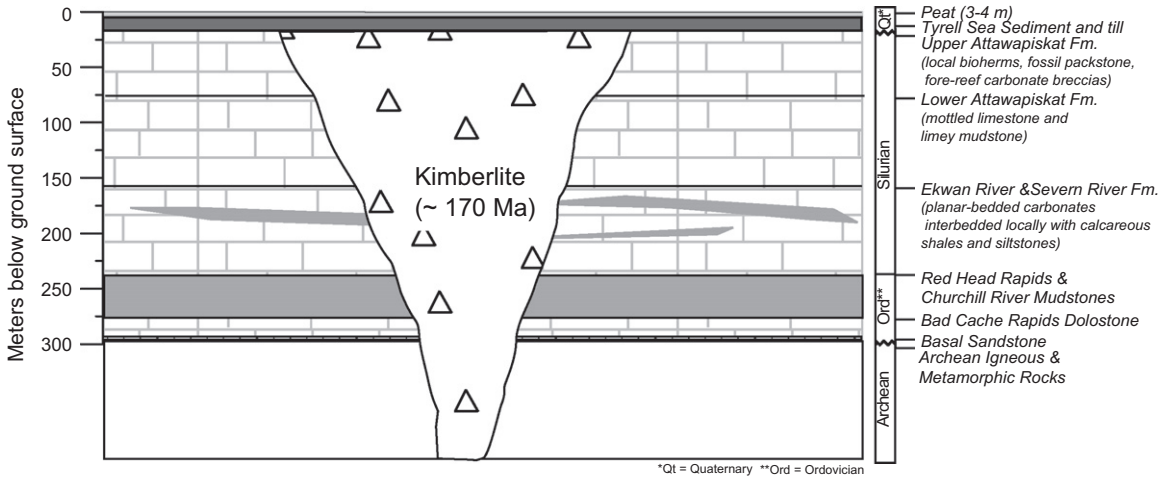

Fig. 2. Schematic vertical section of rocks and sediment in which Attawapiskat kimberlites are emplaced. Kimberlite and host rocks are overlain by a thin till, Tyrell Sea sediment (10–5 ka), and peat (5 ka to present). Geology from Norris (1993).

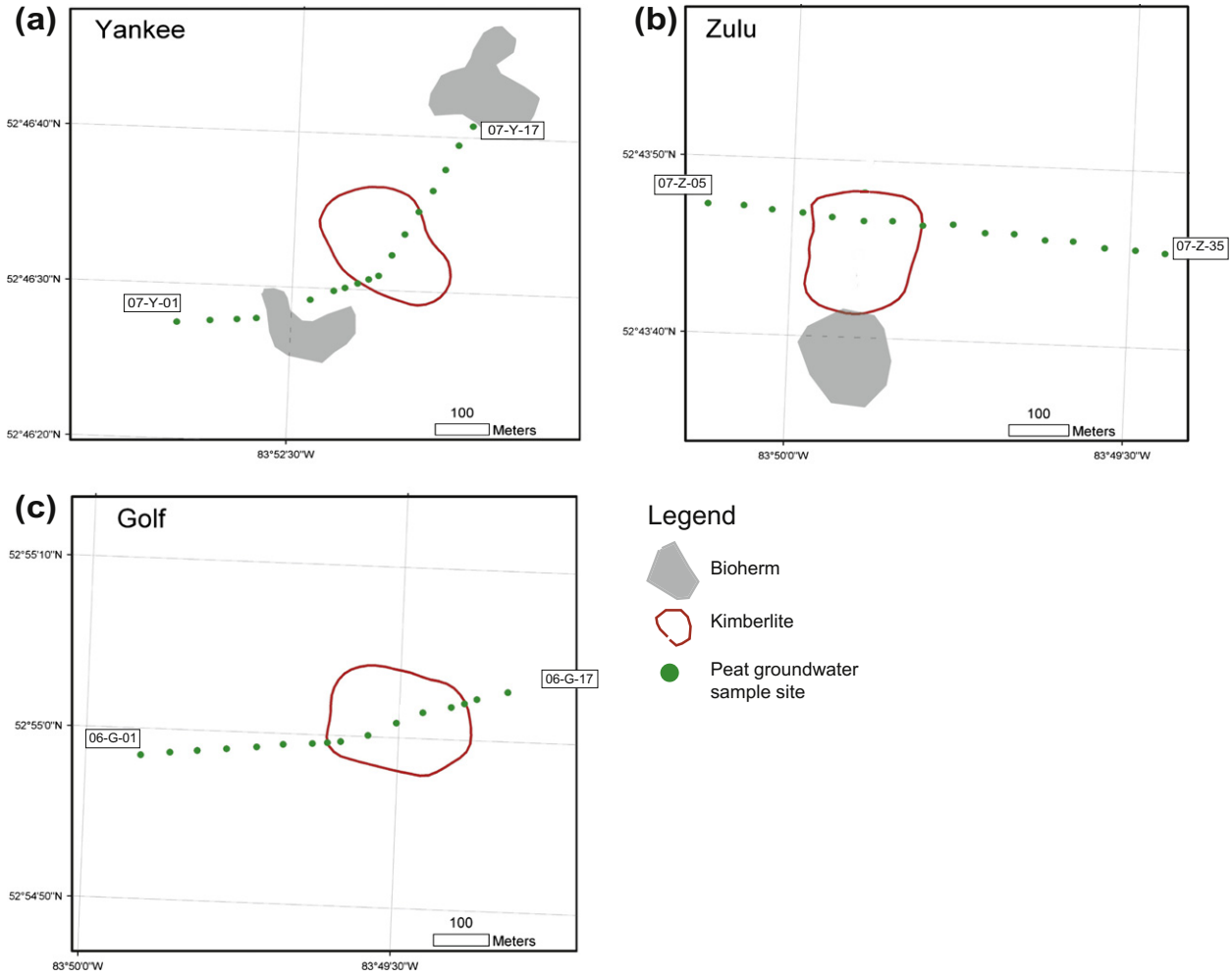

Fig. 3. Location of the (a) Yankee, (b) Zulu, and (c) Golf kimberlites, and peat groundwater sample sites. The aerial extent of each kimberlite was determined using geophysical data and exploration drilling by DeBeers Canada. Figures modified from Sader et al. (2011).

gradient at both Yankee and Zulu indicates peat groundwater generally flows from west to east. The flow rate ranges from a minimum of approximately 2 cm/a to a maximum of 200 cm/a at a sample depth of 1.1 m below ground surface (mbgs). The upwelling of deep minerotrophic groundwaters into peat was recognized by observation of a higher potentiometric surface in deeper monitoring wells installed in the TSS compared with the water table elevation measured in the piezometers installed in

Table 1
Geochemical compositions of peat groundwaters along sampling transects over Yankee and Zulu kimberlites.

Sample	Detection limit	07-Y-01	07-Y-02	07-Y-03	07-Y-04	07-Y-05.5	07-Y-06	07-Y-07	07-Y-08	07-Y-09	07-Y-10	07-Y-11	07-Y-12	07-Y-13	07-Y-14	07-Y-15	07-Y-16	07-Y-17
Distance along transect (m)		0	64	116	153	255	299	324	349	370	393	443	489	539	589	639	689	739
Upwelling groundwater sites		Upwelling	Ombrotrophic	Ombrotrophic	Upwelling	Ombrotrophic	Ombrotrophic	Ombrotrophic	Upwelling	Upwelling	Ombrotrophic	Upwelling	Upwelling	Ombrotrophic	Ombrotrophic	Ombrotrophic	Ombrotrophic	Ombrotrophic
Bedrock substrate		Limestone	Limestone	Limestone	Limestone	Limestone	Limestone	Limestone	Kimberlite	Kimberlite	Kimberlite	Kimberlite	Kimberlite	Kimberlite	Kimberlite	Limestone	Limestone	Limestone
Lat		52.8455	52.7743	52.7743	52.7744	52.7747	52.7749	52.7750	52.7751	52.7751	52.7752	52.7756	52.7760	52.7764	52.7768	52.7771	52.7776	52.7779
Long		−83.7915	−83.8772	−83.8765	−83.8759	−83.8745	−83.8739	−83.8735	−83.8732	−83.8729	−83.8726	−83.8723	−83.8720	−83.8716	−83.8712	−83.8709	−83.8706	−83.8702
Temp °C		8.7	9.8	9.0	9.5	8.8	8.1	7.9	7.7	6.3	7.4	6.7	8.2	10.4	8.0	7.2	7.6	4.2
pH		5.49	5.87	5.89	7.71	6.41	5.59	5.77	7.15	6.53	6.21	7.37	6.83	5.71	6.40	6.11	6.21	7.10
Eh (mV)		332	316	316	260	303	317	316	240	299	316	224	258	325	266	303	294	302
EC (μS/cm)		29	56	55	264	92	55	47	218	78	30	301	71	35	45	30	41	54
DO (mg/L)		1.24	2.23	3.11	4.47	4.48	4.39	2.56	2.72	1.72	1.90	2.66	1.19	4.00	1.97	0.77	8.00	3.13
DIC (mg/L)		7.36	na	15.31	36.00	22.67	na	11.68	30.30	20.37	9.82	47.88	25.61	10.14	13.66	19.05	12.95	na
DOC (mg/L)		38.80	na	57.74	25.00	39.72	na	67.57	25.64	106.78	45.46	25.62	28.42	43.98	47.38	60.21	59.68	35.62
Carbonate Alk. (mg/L)		0	20	30	142	na	50	0	0	119	76	0	183	82	0	0	0	0
mg/L																		
Ca	0.03	2.91	7.07	8.12	60.54	17.89	9.15	5.75	26.18	21.12	5.49	63.91	14.01	2.52	3.43	3.36	6.50	9.54
Mg	0.01	0.24	0.33	0.31	0.88	0.68	0.81	0.59	12.55	2.04	0.38	2.84	0.45	0.34	0.49	0.46	0.48	0.44
K	0.18	0.35	0.36	bd	bd	0.26	bd	bd	bd	0.31	bd	bd	bd	0.25	0.45	0.26	0.19	0.27
Na	0.05	0.34	0.44	0.36	0.42	0.80	0.52	0.39	0.66	0.47	0.26	0.85	0.33	0.34	0.33	0.44	0.43	0.50
SO_4^{2-}	0.04	0.36	na	0.21	0.39	0.04	na	0.29	1.09	0.09	0.15	0.07	0.12	0.39	0.38	3.97	0.33	na
Cl^-	0.03	0.59	na	0.76	0.63	0.12	na	1.24	0.71	0.89	0.71	0.87	0.22	2.05	1.2	0.73	1.68	na
μg/L																		
Fe	3	155	409	258	25	302	256	171	400	586	111	4052	4726	119	140	151	448	1428
Mn	1	18	23	7	65	6	14	33	78	34	17	74	129	19	12	14	36	26
Al	5	157	81	74	28	33	69	141	156	135	84	12	14	66	133	100	121	79
S	300	318	bd	bd	510	bd	348	bd	467	bd	bd	433	bd	341	bd	358	373	394
Cr	0.02	0.32	0.11	0.14	0.09	0.09	0.19	0.24	4.23	0.20	0.18	0.24	0.13	0.25	0.22	0.35	0.48	0.34
Ba	0.02	2.80	2.62	2.69	3.11	4.25	3.04	3.26	58.06	8.65	2.41	8.57	6.41	1.71	2.11	2.00	3.05	2.92
Ni	0.10	0.40	0.40	0.42	0.66	0.51	0.46	0.87	60.76	1.22	0.56	1.87	0.40	0.35	0.42	0.51	1.18	0.64
Rb	0.005	0.717	1.009	0.193	0.240	0.670	0.363	0.176	0.553	1.002	0.446	0.481	0.260	0.498	0.624	0.540	0.599	0.586
Nd	0.003	0.031	0.035	0.031	0.092	0.026	0.051	0.054	0.823	0.056	0.040	0.039	0.009	0.032	0.028	0.048	0.064	0.034
Cu	0.2	18.8	1.9	1.3	0.8	1.8	3.1	7.5	3.2	2.6	4.0	5.1	3.0	3.4	2.9	5.3	9.7	3.9
Zn	1	18.9	4.0	3.3	1.6	6.1	7.0	11.7	1.7	7.9	5.9	6.4	6.3	21.8	5.0	8.2	10.9	7.3
Sr	0.1	3.67	7.22	7.20	43.32	20.05	9.17	6.53	137.55	23.88	5.23	46.69	11.32	2.84	3.60	3.98	6.07	7.95
Y	0.0005	0.0215	0.0212	0.0247	0.0895	0.0227	0.0352	0.0324	0.3144	0.0408	0.0304	0.0483	0.0071	0.0313	0.0629	0.0294	0.0382	0.0348
Pb	0.05	0.52	0.66	0.53	0.10	0.38	1.28	0.98	0.17	0.59	0.72	0.39	0.22	0.30	0.47	0.40	0.81	0.32

Sample	Detection limit	07-Z-05	07-Z-07	07-Z-09	07-Z-11	07-Z-13	07-Z-15	07-Z-17	07-Z-19	07-Z-21	07-Z-23	07-Z-25	07-Z-27	07-Z-29	07-Z-31	07-Z-33	07-Z-35
Distance along transect (m)		0	50	100	150	200	250	300	350	400	450	500	550	600	650	700	750
Upwelling groundwater sites		Ombrotrophic	Ombrotrophic	Ombrotrophic	Ombrotrophic	Ombrotrophic	Ombrotrophic	Upwelling	Upwelling	Upwelling	Upwelling	Upwelling	Upwelling	Upwelling	Upwelling	Upwelling	Upwelling
Bedrock substrate		Limestone	Limestone	Limestone	Kimberlite	Kimberlite	Kimberlite	Kimberlite	Limestone	Limestone	Limestone	Limestone	Limestone	Limestone	Limestone	Limestone	Limestone
Lat		52.7298	52.7297	52.7297	52.7297	52.7296	52.7296	52.7296	52.7295	52.7296	52.7294	52.7294	52.7294	52.7294	52.7293	52.7293	52.7292
Long		−83.8354	−83.8345	−83.8338	−83.8331	−83.8324	−83.8316	−83.8309	−83.8301	−83.8294	−83.8286	−83.8279	−83.8271	−83.8264	−83.8256	−83.8249	−83.8241
Temp °C		11.2	12.0	9.7	10.8	11.0	9.9	10.0	11.2	9.1	6.5	8.9	9.7	10.1	9.6	4.6	10.5
pH		5.90	5.60	5.27	5.46	5.27	5.41	5.90	6.15	6.44	6.06	5.74	5.77	5.90	6.21	6.39	5.93
Eh (mV)		257	291	327	313	325	310	267	125	190	224	242	239	232	198	190	183
EC (μS/cm)		159	88	38	45	31	35	90	229	168	280	271	154	399	379	303	349
DO (mg/L)		bd	0.57	1.00	0.00	0.13	bd	bd	bd	bd	bd	bd	0.29	0.31	0.57	bd	0.32
DIC (mg/L)		35.56	31.65	26.72	20.16	17.97	19.63	25.39	51.61	38.50	49.85	56.45	43.91	70.10	65.99	54.47	55.44
DOC (mg/L)		56.78	76.84	63.98	66.85	54.14	47.80	132.21	35.81	31.30	26.40	26.50	na	22.47	18.63	18.55	21.40
Carbonate Alk. (mg/L)		63	23	0	0	0	0	75	136	131	142	130	99	216	243	237	214
mg/L																	
Ca	0.03	28.28	17.52	6.82	9.11	3.04	2.52	21.52	38.74	19.23	29.07	38.55	22.00	55.23	62.80	45.15	54.76
Mg	0.01	0.65	0.58	0.34	0.60	0.81	0.56	3.77	6.35	5.19	7.26	7.63	5.22	11.88	13.19	8.62	8.80
K	0.18	0.37	bd	0.27	bd	0.43	bd	0.50	2.51	2.62	2.48	1.78	2.65	2.22	1.63	1.03	0.81
Na	0.05	1.05	0.60	1.14	0.75	1.06	0.35	3.32	12.54	11.40	20.99	14.07	11.02	28.55	25.51	30.59	25.80

Table 1 (*continued*)

Sample	Detection limit	07-Z-05	07-Z-07	07-Z-09	07-Z-11	07-Z-13	07-Z-15	07-Z-17	07-Z-19	07-Z-21	07-Z-23	07-Z-25	07-Z-27	07-Z-29	07-Z-31	07-Z-33	07-Z-35
SO_4^{2-}	0.04	0.22	0.21	0.25	0.23	0.40	0.20	0.27	0.53	0.20	0.22	0.80	0.20	0.17	0.22	0.22	0.29
Cl^-	0.03	1.81	0.81	1.20	1.60	1.05	0.81	0.28	2.52	1.67	2.02	2.69	2.71	14.60	16.84	25.43	18.72
µg/L																	
Fe	3	1507	1111	513	622	261	138	526	235	249	1042	1609	877	2235	3588	2763	3551
Mn	1	18	17	8	10	10	6	17	25	6	22	30	54	80	112	40	91
Al	5	46	72	58	64	59	67	79	13	365	6	7	13	6	10	9	23
S	300	bd	332	bd	bd	bd	bd	328	bd	bd	bd	bd	bd	bd	bd	bd	bd
Cr	0.02	0.10	0.10	0.24	0.13	1.14	0.40	0.25	0.32	0.13	0.08	0.20	0.13	0.07	0.21	0.08	0.10
Ba	0.02	7.60	3.66	3.32	3.29	7.80	6.31	20.72	49.97	18.49	12.83	15.89	10.29	16.90	14.07	12.62	14.57
Ni	0.10	0.35	0.67	0.41	0.33	1.42	0.62	1.05	1.15	0.24	0.31	0.27	0.34	0.17	0.26	0.46	0.43
Rb	0.005	0.795	0.352	0.605	0.149	0.831	0.202	0.497	2.638	2.184	2.223	1.831	3.435	1.491	1.297	0.822	0.550
Nd	0.003	0.033	0.026	0.043	0.032	0.036	0.053	0.055	0.035	0.018	0.014	0.010	0.017	0.006	0.007	0.009	0.023
Cu	0.2	1.0	0.7	4.0	1.3	9.8	6.0	6.8	3.0	3.0	0.9	3.9	1.9	1.2	3.2	0.9	1.5
Zn	1	8.6	2.6	6.2	2.6	20.3	7.7	7.7	16.3	4.9	12.5	10.9	6.6	1.8	10.7	2.4	3.0
Sr	0.1	39.87	22.84	12.25	14.08	8.02	8.82	71.62	164.01	90.54	117.39	127.93	69.79	191.83	203.05	128.19	125.35
Y	0.0005	0.0208	0.0184	0.0220	0.0246	0.0298	0.0312	0.0357	0.0193	0.0135	0.0083	0.0090	0.0096	0.0088	0.0170	0.0093	0.0173
Pb	0.05	0.24	0.43	0.81	0.47	1.25	1.22	1.08	0.39	0.65	0.17	0.22	0.16	0.09	0.17	0.13	0.18

na = not analysed.
bd = below detection.

peat. In peat groundwater samples, the pH values vary from 3.80 to 7.10 and Eh values range from 125 to 512 mV. High pH and low Eh values are generally observed in the presence of upwelling groundwater along each transect. Samples from the Golf transect, as a whole, have the most oxidized peat groundwater conditions (lowest pH and highest Eh values), likely a result of the shallow (0.4 mbgs) water collection depth. Peat groundwater electrical conductivity (EC) values are highly variable and are elevated at sites of upwelling deep groundwater. High EC values are commonly used to identify sites of upwelling minerotrophic groundwaters in wetlands (Hill and Siegel, 1991; Hoag and Price, 1995; Ingram, 1983). Boelter and Verry (1977) define EC values in peat groundwaters up to 80 µS/cm as being ombrotrophic and values greater than 100 µS/cm as having a contribution from minerotrophic groundwaters. In this study, ombrotrophic conditions are defined as those with EC values less than 100 µS/cm and peat groundwaters with minerotrophic groundwater contributions as those with EC values greater than 100 µS/cm. The greater the EC value, the greater the minerotrophic groundwater contribution.

Based on the combination of hydrogeological and geochemical peat groundwater data in Sader et al. (2011), upwelling occurs as isolated point sources at 0, 153, 349, 370 and 489 m along the Yankee transect and near the kimberlite margin at 300 m, extending to the east end of the Zulu transect. Upwelling occurs between sites at 300 and 400 m and extends to the east end of the Golf sampling transect.

3. Methods

3.1. Field procedures

Peat groundwater samples were collected during the summers of 2006 (early August) and 2007 (August 14–23) along transects over the Yankee, Zulu, and Golf kimberlites. Samples collected in 2006 and 2007 are denoted by the prefixes 06 and 07, respectively. Samples along Yankee, Zulu, and Golf transects are denoted by the prefixes Y, Z, and G, respectively. All geochemical data for water samples collected in 2006 are from Brauneder (2007). The compositional data for water samples collected in 2007 are presented in Table 1.

Field sampling methods from Sader et al. (2011) for peat groundwaters are summarized below. Shallow piezometers used for peat groundwater sampling were constructed from 1.5 m lengths of either 19 mm (¾ inch) inner diameter white (environmental grade) or grey polyvinyl chloride (PVC) piping. Piezometers were installed 1.1 mbgs into the peat along sampling transects across the Yankee and Zulu kimberlites, and 0.4 mbgs along the Golf kimberlite transect. Shallow piezometers were installed approximately every 25–50 m along each sampling transect and at least 200 m beyond the kimberlite margins where possible (Fig. 3). Peat groundwater samples were collected from each of the installed piezometers.

The pH, oxidation–reduction potential (ORP), electrical conductivity, dissolved O_2 content (DO), and temperature were measured on-site with a Hanna™ HI-9828 multi parameter water quality portable meter. Probes for pH, DO, and EC were calibrated daily. ORP values have been corrected to the standard hydrogen electrode (SHE) for waters at 10 °C by adding 207 mV, and are reported as Eh.

Water samples were filtered through Millipore™ 0.45 µm filters into 60 and 30 mL Nalgene high-density polyethylene (HDPE) bottles for cation and anion analysis, respectively. Samples for dissolved inorganic C (DIC) and dissolved organic C (DOC) analysis were collected in 40 mL brown borosilicate bottles with a silicone–polytetrafluoroethylene (PTFE) septa cap. An additional PTFE

and rubber septa from Chromatographic Specialties Inc. was inserted underneath the septa cap to prevent DIC loss (silicone is gas permeable). All water samples were kept cool in ice-packed coolers or refrigerated until they were analyzed. Prior to analysis water samples for cation analysis were acidified to 1% using Baseline-grade HNO_3 from Seastar Chemicals.

3.2. Laboratory procedures

Concentrations of DIC and DOC in waters were determined at the University of Ottawa G.G. Hatch Stable Isotope Laboratory using a Finnigan-Mat Delta Plus mass spectrometer and the 2σ analytical precision is ±0.002 ppm. Elemental analyses of groundwaters for cations and anions were conducted at the Geoscience Laboratories, Ontario Ministry of Northern Development of Mines, Sudbury, Canada. Calcium, Fe, K, Mg, Mn, Na and S were determined by ICP-ES; Ti, Cr, Ni, Rb, Sr, Nd, Ba, Cu, Zn, and Y were determined by ICP-MS; and Cl^- and SO_4^{2-} were determined by IC. A precision of <5% RSD was achieved for all metals and anions with the exception of Mn (7%), Zn (6%) and Ti (11%). A full description of cation and anion analytical procedures including quality assurance and quality control procedures, have been reported elsewhere (Sader et al., 2011).

3.3. Speciation calculations and modeling

The nonideal competitive adsorption model (NICA) and Donnan database in Visual MINTEQ 3.0 (Gustafsson, 2010), was used to calculate Nd, Ni, Ba and K complexation with DOM. This model is based on the combination of two active processes. The NICA model simulates metal complexation and was first developed by Koopal et al. (1994). This model assumes that binding sites to humic substances are heterogeneous and treats them as continuous functions. It also takes into consideration competition effects between metals and other ions in the solution, which is represented by ionic strength. The Donnan database model (Benedetti et al., 1996) concerns electrostatic interactions of ions and assumes that the dissociation of carboxylic and phenolic groups results in an electrical potential around those substances and that organic matter is in a gel phase. The negative charge around these molecules exerts a binding effect for ions (Kinniburgh et al., 1999).

The Visual MINTEQ model assumes that DOM consists of 50% C (Thurman, 1985). Of the total DOM, 70% is considered fulvic acid and the other 30% is considered inert organic acids (i.e., acetic acid) that do not contribute to metal complexation (Bryan et al., 2002). Visual observation of peat groundwater samples in this study indicated they were colourless and suggest fulvic acid is likely the dominant organic acid, as humic acids are darker in colour (Stevenson, 1994). Acidification of peat groundwater samples to ~1 pH for cation analysis did not result in humic acid precipitation in all but two samples also suggesting fulvic acids are dominant. Humic acids are only soluble at pH > 2, whereas fulvic acids are soluble throughout the pH range. Although it is possible there are some humic acids in peat groundwater samples, modeling calculations with only fulvic acid is not expected to markedly influence the model's ability to predict metal–DOM speciation. Other studies modeling metal–DOM complexation with fulvic acid only (i.e., Astrom et al., 2010; Bryan et al., 2002; Dwane and Tipping, 1998; Ronnback et al., 2008) have shown that modeling results were in good agreement with analytical results of metal–DOM complexation in a variety of natural waters.

The binding constants (logK) used in this model calculation for Ni and Ba are from Milne et al. (2003) and are in the Visual MINTEQ – NICA-Donnan database. The binding of K in the model is calculated based on the Donnan database only and relates to attraction between the negatively charged DOM and counterions (free metal ions). Potassium is not favored to form strong bonds with DOM, and thus is not considered in the NICA database. The logK values for Nd, derived by Sonke and Salters (2004), were added separately, as they are not included in the original database.

Visual MINTEQ was used to calculate the fraction of dissolved metals that adsorbed on ferrihydrite. The *feo-dlm_2008.vdb* database uses the 2-pK Diffuse Layer Model. Dzombak and Morel (1990) derived the ferrihydrite surface complexation constants for Ni and Ba. Because a constant for Nd was not included in the database, an experimentally derived constant for Nd from Tang and Johannesson (2005) was used. No constant was available for K, however, it has little affinity to adsorb on ferrihydrite surfaces (Kinniburgh et al., 1976). The Dzombak and Morel (1990) model assumes that ferrihydrite has a surface area of 600 m^2/g. The model also assumes the ferrihydrite is 89 g/mol; 17.8 g/mol have weak sites and 0.445 g/mol have strong binding sites.

In Visual MINTEQ, concentrations of ferrihydrite were set at 1 g/L for sites with low contributions from upwelling groundwaters (EC < 100 μS/cm) and 10 g/L at sites of upwelling minerotrophic waters (EC > 100 μS/cm). These ferrihydrite concentrations were chosen because total Fe contents in peat reported by Hattori and Hamilton (2008) along the same Yankee and Golf transects as this study ranged from 0.05% to 0.15% where EC was <100 μS/cm and ranged from 0.7% to 3.19% where EC was >100 μS/cm. It is assumed that the majority of total Fe exists as secondary precipitated ferrihydrite because no residual mineral grains were visually identified in the peat. For Zulu model calculations, the ferrihydrite content at sites 300, 350 and 400 m were set at 1 g/L and at sites 450–750 m the content was set at 10 g/L. For Golf, ferrihydrite content was set at 1 g/L at sites 309–569 m and at sites 594–722 m it was set at 10 g/L.

Table 1 lists the dissolved metal concentrations and geochemical parameters from Yankee and Zulu peat groundwaters that were input into the NICA-Donnan and ferrihydrite surface complexation models. The geochemical data for Golf are from Brauneder (2007).

4. Results

4.1. Peat groundwater geochemistry

Dissolved organic C concentrations range from 15.8 to 132.2 mg/L. They are elevated (>40 mg/L) in peat groundwaters that receive little to no contribution from upwelling minerotrophic groundwater (EC < 100 μS/cm). The low DOC concentrations (<40 mg/L) are generally associated with sites that have high contributions from upwelling minerotrophic groundwater (EC > 100 μS/cm). Transition metals such as Ni, Ti, Cr and Nd are elevated with concentrations up to 1.8, 4.0, 1.1 and 0.10 μg/L, respectively, in peat groundwaters at or near kimberlite margins compared to baseline Attawapiskat peat groundwater concentrations (Figs. 4 and 5). The exception is site 349 m (07-Y-08) at Yankee, which has transition metal concentrations that are 4–60 times greater and are more similar to groundwaters from the TSS (Sader et al., 2011). The elevated values are notably higher than local baseline values in ombrotrophic peat groundwaters. Collectively, peat groundwaters from all sites show that increases in Ni, Ti, Cr and Nd concentrations correlate with increases in DOC, where EC is lower (Fig. 4).

Concentrations of the alkaline earth metals Mg and Ca decrease with increasing concentrations of DOC (Fig. 4), due to high Mg and Ca concentrations (up to 13.2 and 62.8 mg/L, respectively) and low DOC concentrations common in upwelling minerotrophic groundwaters. Magnesium and Ca increases with increasing EC (Fig. 4) are also a function of the geochemistry of upwelling minerotrophic groundwaters. At most sampling sites high Mg and Ca reflect upwelling regardless of whether the waters are spatially related

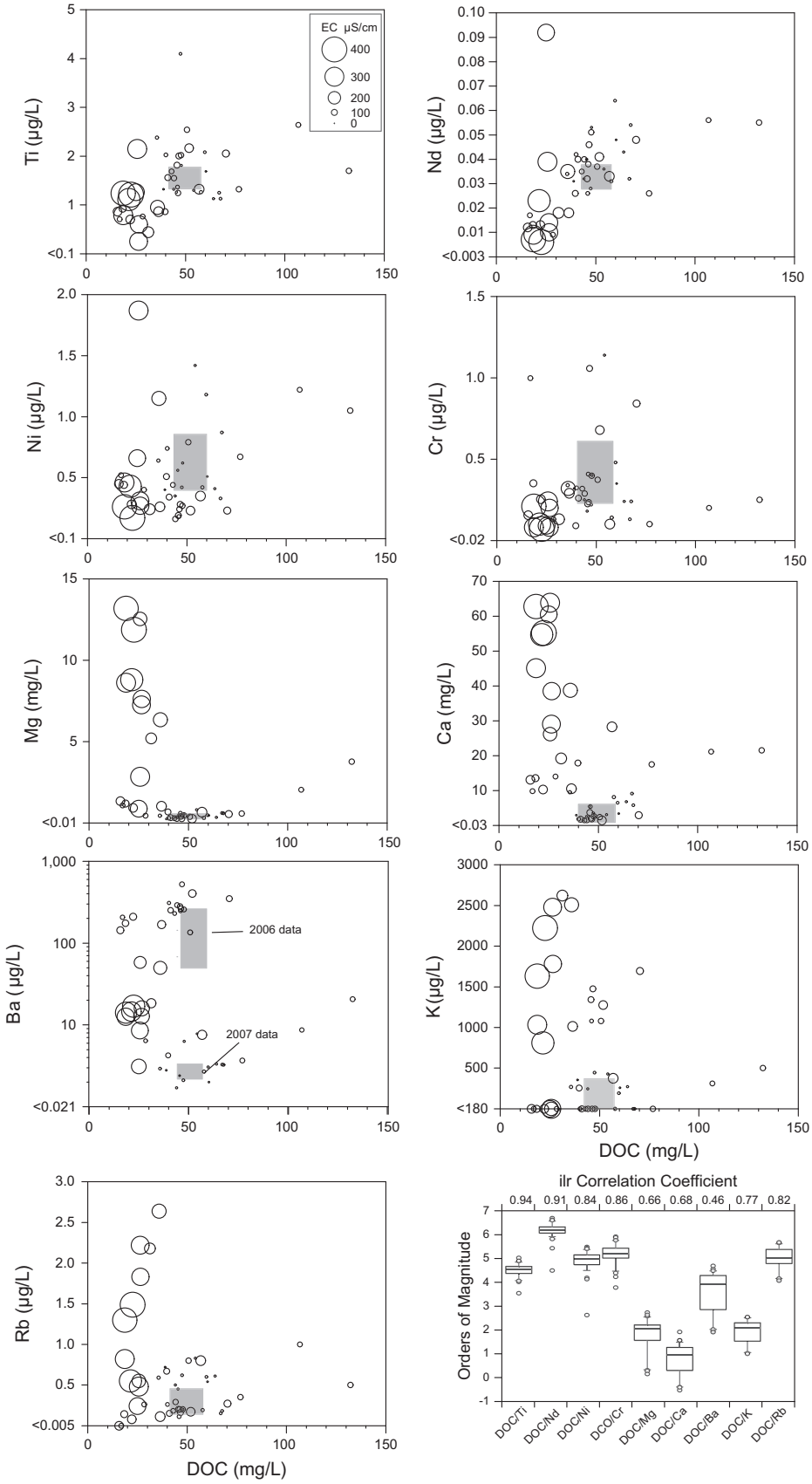

Fig. 4. DOC versus major, minor and trace elements in peat groundwaters for Yankee, Zulu, and Golf kimberlites (n = 50). Increases in DOC and decreases in EC coincide with increased concentrations of Ti, Nd, Ni and Cr. Concentrations of Mg, Ca, Ba, K and Rb display the opposite trend. Boxes within the scatter plots represent the first and third quartile values for baseline ombrotrophic peat groundwaters with respect to metals and DOC. Note that there are two box plots for Ba; one for 2006 data and one for 2007 data. The ilr transformation for DOC/metals (see Eq. (1)) in the bottom right corner is represented by box plots, which include the median, first and third quartile values, and outliers. Transition metals tend to have the highest ilr correlation coefficient (see Eq. (2)).

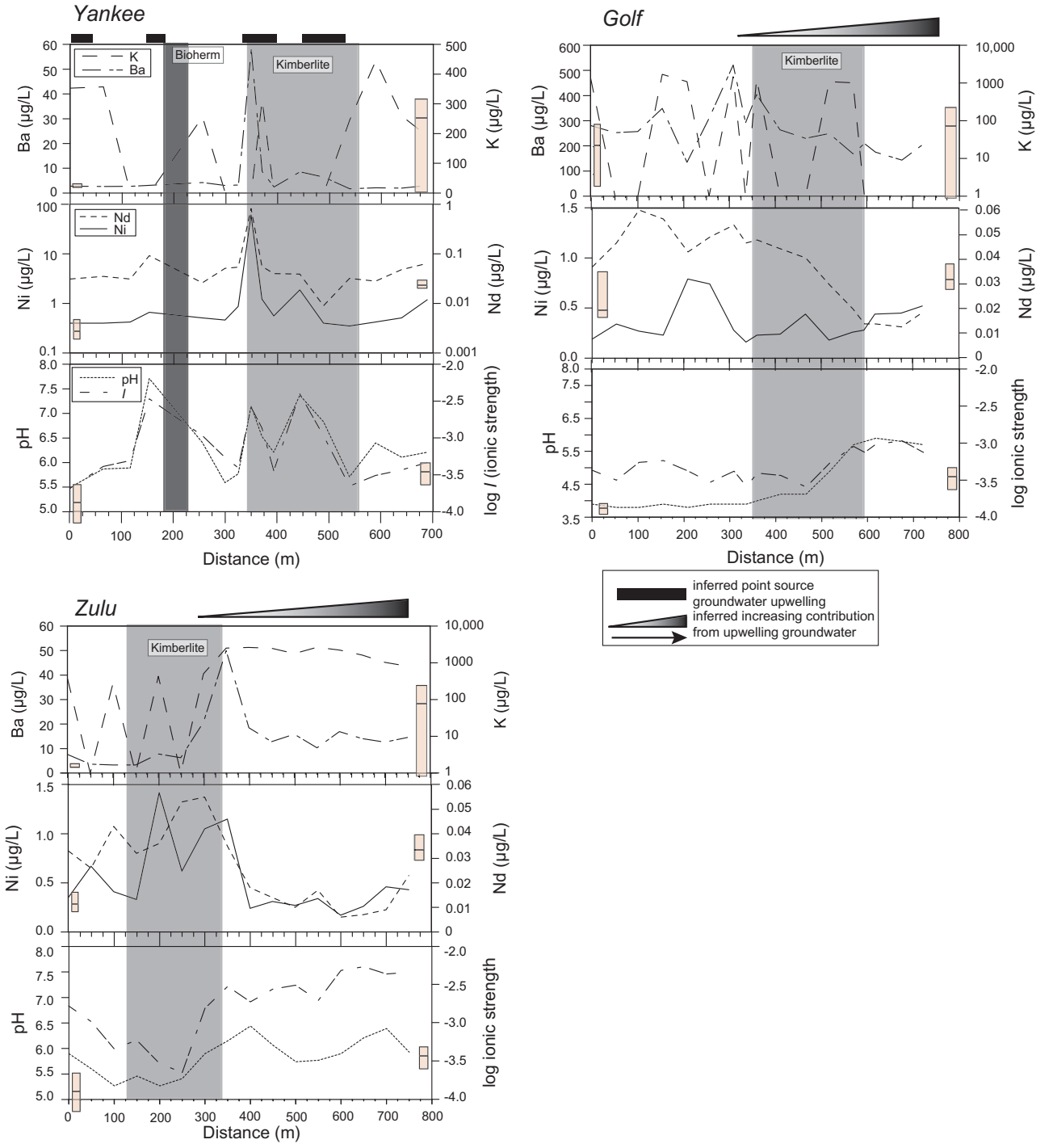

Fig. 5. Profiles of peat groundwater Ba, K, Ni, Nd, pH and ionic strength (*I*) along transects over Yankee, Zulu and Golf kimberlites. Data for Golf is from Brauneder (2007). Box plots represent the median, first and third quartile values for baseline ombrotrophic peat groundwaters.

to locations of buried kimberlite. Concentrations of alkali metals such as K and Rb are commonly elevated at sites with elevated EC and low DOC (Fig. 4).

Elevated Ba concentrations (10–50 µg/L) also reflects upwelling groundwater (Fig. 4), however, unlike the majority of Mg or Ca, the greatest concentrations are located at sites at or near the kimberlite margins. Note that the Ba concentrations at Golf are two orders of magnitude greater than Yankee or Zulu. All waters collected during summer 2006 have high Ba values (Brauneder, 2007). Although the reason is not known, the possibility of contamination, or analytical artifact have been ruled out. Laboratory QA and QC results indicated a relative standard deviation (RSD) of <5% for Ba, and analytical runs for Ba using ICP-MS and ICP-AES had almost identical concentrations. Furthermore, Ba concentrations in peat groundwaters from 2006, which were collected at 0.4 mbgs along the Yankee transect, had a similar profile shape compared with the Yankee profile in this study (2007 data).

Isometric logratio (ilr) data transformations for the ratio of DOC to metals were calculated using equation:

$$\mathrm{ilr} = \log(x_1/x_2) \quad (1)$$

based on work conducted by Filzmoser et al. (2010). For a given groundwater sample x_1 is the DOC concentration and x_2 is the metal concentration. The correlation coefficient of the ilr values were then computed using the equation:

$$\mathrm{corr}(x_1, x_2) = \exp(-\mathrm{var}(\mathrm{ilr})) \quad (2)$$

where var(ilr) is the variance of z (Filzmoser et al., 2010). This correlation gives an indication of the stability of the ratio between DOC and metal concentrations in peat groundwater. A correlation coefficient closer to 1 indicates low variability in the ilr (DOC and metals in the sample set have similar log ratios) and a correlation coefficient closer to 0 indicates high variability in the ilr. The ilr correlation coefficients for Ti, Nd, Ni and Cr versus DOC, are strong (0.94, 0.91, 0.84 and 0.85, respectively; Fig. 4). In comparison, the ilr correlation coefficients for Mg and Ca versus DOC are lower (0.66 and 0.68, respectively; Fig. 4), due to the variability in mixing of minerotrophic upwelling groundwater and ombrotrophic peat groundwater. The ilr correlation coefficients for K and Rb versus DOC are 0.77 and 0.82, respectively, indicating that most of the K and Rb concentrations are less variable with DOC concentrations compared to Mg and Ca. Because of the variability of Ba concentrations (two orders of magnitude between 2006 and 2007 data), the ilr correlation coefficient is low (0.46; Fig. 4).

Alkaline earth metals, specifically Ca and Mg, strongly contribute to ionic strength (I) values in peat groundwater and the correlation between Ca + Mg and ionic strength is strong ($r = 0.98$). Elevated log$I$ values (-3 to *c.* -2) are present due to elevated dissolved metal inputs from upwelling groundwater along each of the three sampling transects (Fig. 5). Sulfate concentrations are low at all sites (mean = 0.35, median = 0.3, max = 3.97 mg/L); and total S concentrations in waters are also low (mean = 0.4, max = 0.9, with many samples less than the detection limit of 0.3 mg/L) (Table 1). Chloride concentrations are low and range from 0.12 to 25.4 mg/L with mean and median concentrations of 3.6 and 2.0 mg/L, respectively.

4.2. Geochemical model calculations

4.2.1. Metal speciation calculations

Dissolved metals were calculated as organic complexes, inorganic complexes and free ions. The model calculations indicate that aqueous metal–sulfate species are low and comprise less than 2% of total dissolved metals in all groundwater conditions (ombrotrophic or minerotrophic) (Fig. 6). The metal–carbonate complexes are generally ⩽1% at sites with ombrotrophic peat groundwaters (Fig. 7). However, modeled Ni and Nd–carbonate complexes are around 10% at sites of upwelling, and can be has high as 60% at select sites of upwelling at Yankee (Fig. 7). High calculated metal–carbonate complexes are a function of the increases in alkalinity associated with minerotrophic groundwaters (Table 1).

Metal–DOM complexation calculations were conducted using Visual MINTEQ for Nd, Ni, Ba and K in peat groundwater samples along the Yankee, Zulu and Golf transects. These four metals were selected as they represent kimberlite pathfinder metals that are high in peat and peat groundwaters overlying kimberlites relative to sites distal to kimberlites in the Attawapiskat kimberlite field (Hattori and Hamilton, 2008; Sader et al., 2011). They are also of different metal groupings. Neodymium, Ni, and Ba have established NICA-Donnan binding constants (Milne et al., 2003; Sonke and Salters, 2004). Although Rb and Ti are considered kimberlite pathfinder metals, they are not modeled due to the lack of available binding constants in either the NICA or Donnan databases. Binding constants are available for Cr (Milne et al., 2003), however Cr was not modeled, as Khai et al. (2008) indicated there is a large discrepancy between measured and modeled Cr. They suggested this discrepancy is possibly related to the ferrihydrite complexation constant (Dzombak and Morel, 1990), as it is an estimate based on linear free energy.

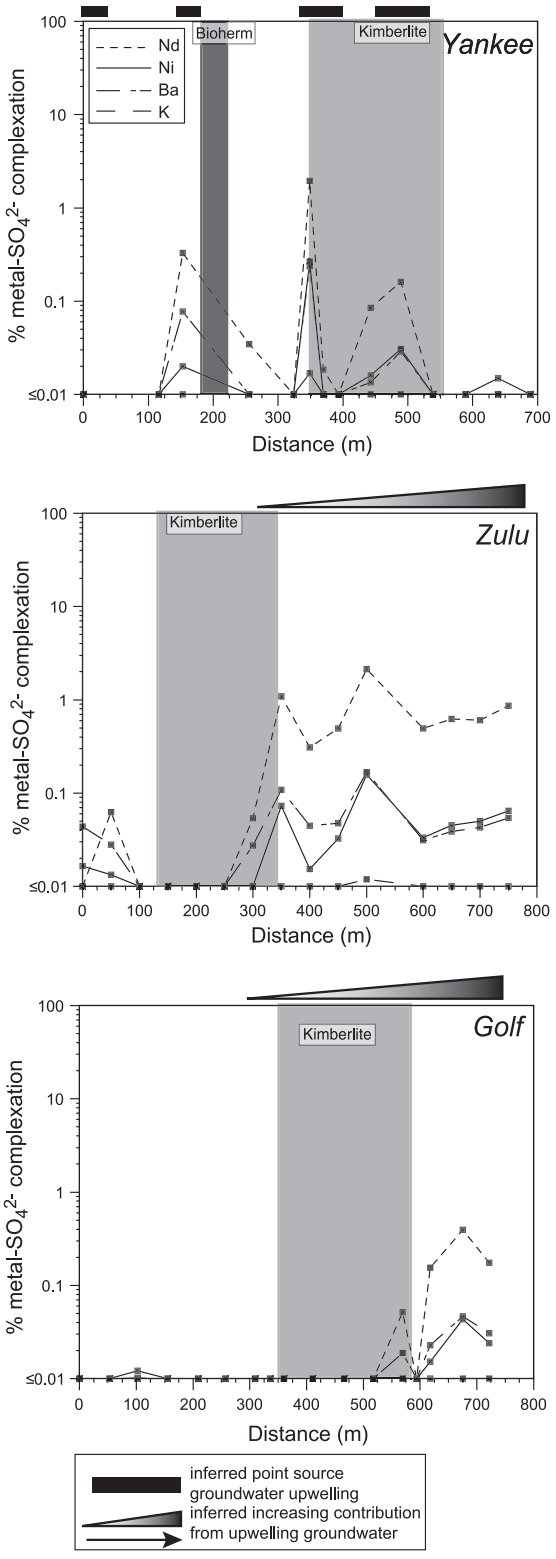

Fig. 6. Profiles of MINTEQ-calculated metal–sulfate species shown as a percentage of total metal content in peat groundwater along transects over Yankee, Zulu and Golf kimberlites.

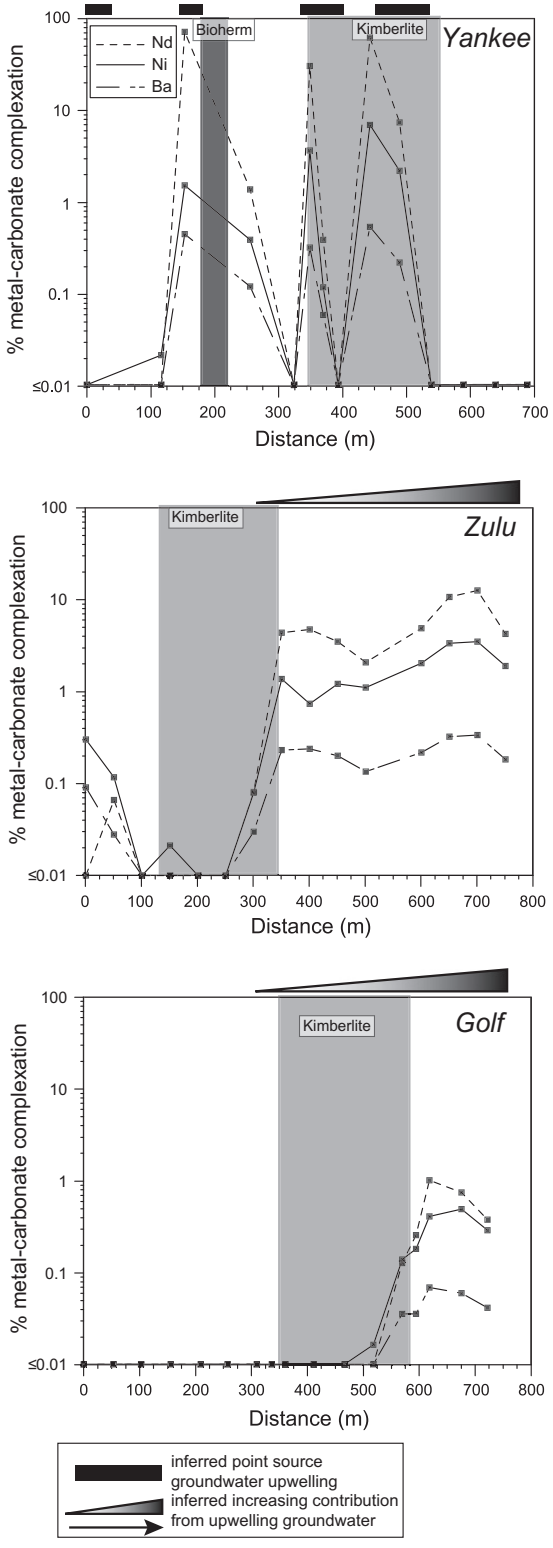

Fig. 7. Profiles of MINTEQ-calculated metal–carbonate species shown as a percentage of total metal content in peat groundwater along transects over Yankee, Zulu and Golf kimberlites. Note that no K-carbonate species are favoured to form in the model.

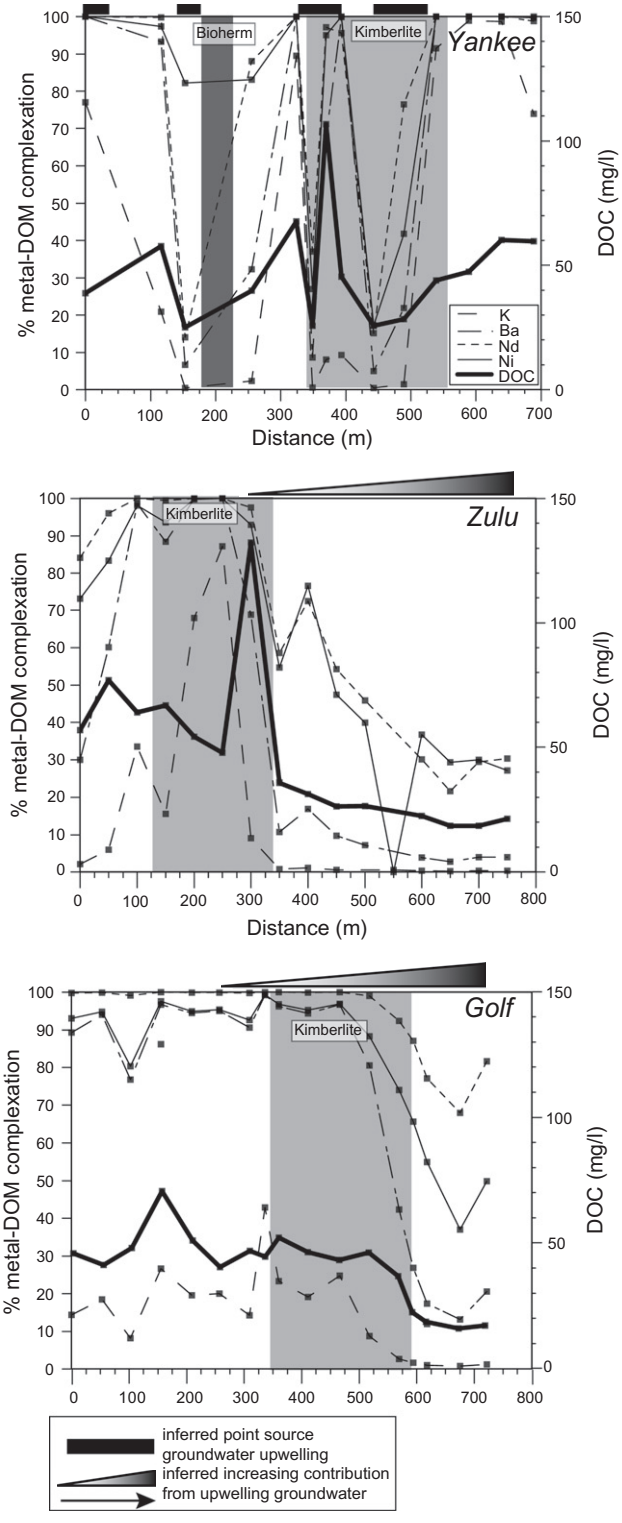

Fig. 8. The profiles of MINTEQ-calculated metal–DOM speciation shown as a percentage of total metal content in peat groundwater along transects over Yankee, Zulu and Golf kimberlites. The profiles indicate that at sites of strong upwelling the fraction of metals bound to DOC decrease.

The fraction of total dissolved metal complexed with DOM along transects at Yankee, Zulu and Golf decreases with decreases in DOC concentrations (Fig. 8), and with increases in pH, and *I* (Fig. 5). Under conditions with little to no contribution from upwelling groundwater, where DOC concentrations are high, pH is low, and *I* is low, almost all soluble Nd, Ni and Ba complex with DOM in peat groundwaters collected along the transects. Under these conditions, a significantly lower fraction of K forms DOM complexes compared with the other metals and is as low as 30% at Golf (Fig. 8).

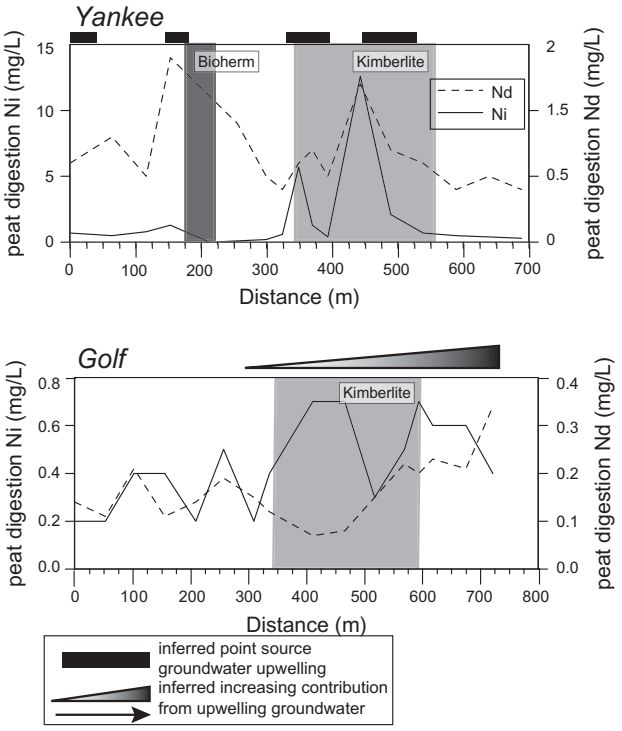

Fig. 9. Profiles of Ni and Nd concentrations in peat total digestions along transects at Yankee and Golf (data from Hattori and Hamilton, 2008). Increased concentrations of Ni and Nd in peat correspond to low concentrations in peat groundwaters (Fig. 5) and lower percentages of metal–DOM complexation (Fig. 8).

At sites of strong groundwater upwelling (lower DOC, higher pH, and higher *I*) the fraction of Nd and Ni bound to DOM decreases. It is generally around 40–50% and sites of upwelling at Yankee are as low as 10%. The fraction of Ba bound to DOM is also lower (15% to <5%), and virtually all K is calculated to exist as free ions. Decreases in the fraction of total Ni and Nd bound to DOM correspond to decreases in the concentration of these metals in the peat groundwater (Fig. 5). However these sites are accompanied by significant increases in concentrations of Ni and Nd in peat total digestion (Hattori and Hamilton, 2008) (Fig. 9). Concentrations of Ba in peat groundwater tend to be elevated at most sites of upwelling located at or near kimberlite margins along Yankee, Zulu, and Golf transects. Potassium concentrations in peat groundwater reflect the fact that alkali metals neither bind strongly to DOM, nor are they strongly scavenged from solution (Fig. 5).

4.2.2. Mineral saturation

Visual MINTEQ was used to calculate ferrihydrite saturation indices ($\log SI_{ferr}$), and calcite saturation indices ($\log SI_{calcite}$) in the presence of DOC for each peat groundwater sample (Fig. 10). Saturation indices were calculated based on the fraction of dissolved Fe^{3+} and Ca^{2+} that were not bound to DOM. The $\log SI_{ferr}$ values are elevated (ca. −5 to 5) at locations which have significant contributions from upwelling minerotrophic groundwaters (EC > 100 μS/cm) (Fig. 10). Typically, the greater the upwelling groundwater contribution, the higher the $\log SI_{ferr}$ values. Overall lower $\log SI_{ferr}$ values along the Golf transect are likely due to the shallower depth of sample collection and more acidic pH. Sites that show strong ombrotrophic characteristics (EC < 100 μS/cm) have lower $\log SI_{ferr}$ values, which range from −5 to −18. Calcite is not predicted to precipitate in any peat groundwaters, as $\log SI_{calcite}$ values for all peat groundwater samples are < 0 (Fig. 10).

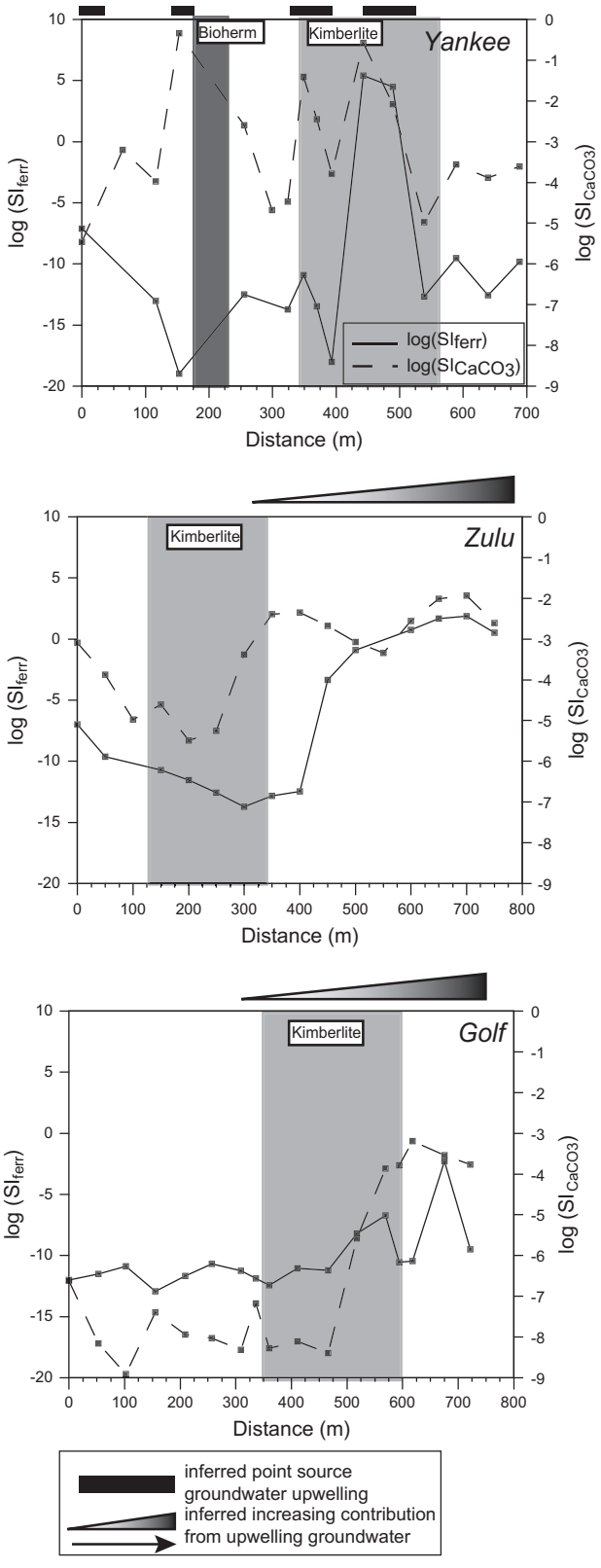

Fig. 10. Profiles of SI_{ferr} and SI_{CaCO3} in peat groundwater at Yankee, Zulu and Golf kimberlites. The highest saturation indices are located at sites along transects which have elevated contributions from upwelling groundwaters. Ferrihydrite is commonly near or greater than saturation at sites of strong upwelling. No samples are saturated with respect to calcite.

4.2.3. Ferrihydrite–metal adsorption calculations

Modeling was conducted to simulate the behaviour of pathfinder metals as peat groundwater geochemistry evolves from

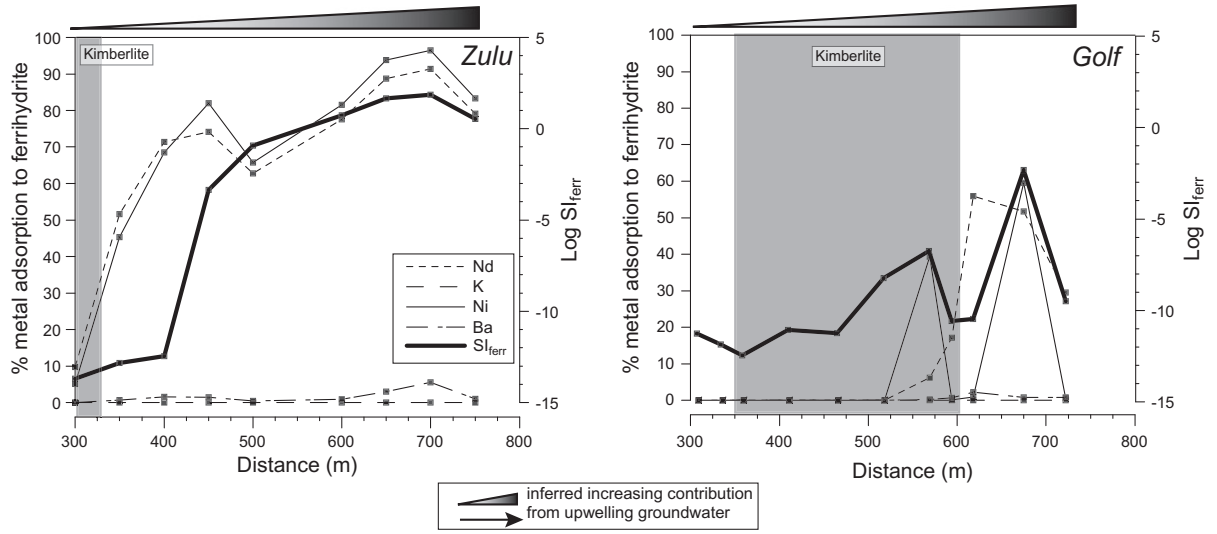

Fig. 11. Profiles of MINTEQ-calculated adsorption of Nd, Ni, Ba and K onto ferrihydrite surfaces along portions of the Zulu and Golf transects starting at 300 and 307 m respectively (sites of increasing contributions from upwelling groundwater). The fraction of Ni and Nd calculated to adsorb to ferrihydrite increases with increasing ferrihydrite saturation indices. Barium and K are not calculated to adsorb strongly to ferrihydrite.

conditions with only minor contributions from upwelling groundwaters to conditions where these contributions dominate. The Zulu and Golf kimberlite transects were used for modeling calculations because they both have progressively greater eastward contributions from upwelling groundwater along their transects starting at site 300, and 307 m at Zulu and Golf, respectively. Pathfinder metal concentrations (Nd, Ni, K and Ba) at Zulu and Golf were held constant and modeled with the geochemical conditions (i.e., pH and Eh), DOC and DIC, and major ions (i.e., Ca, Mg, Na, Fe, Al) observed in successive peat groundwater samples eastward along each transect.

The model calculations indicate progressively greater fractions of Ni and Nd are adsorbed onto ferrihydrite due to peat groundwater geochemistry from increased upwelling groundwater contributions, and thus, increasing ferrihydrite inputs into the model calculations (i.e., 1 or 10 g/L) (Fig. 11). Increasing contributions from upwelling minerotrophic groundwater to the peat has geochemistry that is conducive to the formation of ferrihydrite (higher pH and alkalinity, lower Eh, and greater concentrations of Fe), compared with ombrotrophic peat groundwater. Increases in the Ni and Nd fraction adsorbed to ferrihydrite are roughly inversely proportional to the fraction of dissolved Ni and Nd complexed with DOM and to total dissolved metal concentrations (Figs. 5 and 8). No K and only a small fraction of Ba are calculated to be adsorbed onto ferrihydrite (Fig. 11) and, likewise, there is no relationship with analyzed K and Ba concentrations in peat groundwater (Fig. 5).

5. Discussion

5.1. Controls on metal speciation

Visual MINTEQ calculations indicate the fraction of total dissolved Nd, Ni, Ba and K complexed with DOM in peat groundwaters decreases due to the more minerotrophic geochemistry associated with sites of increased contributions of upwelling groundwaters. The model calculations suggest the binding strength and ion selectivity for DOM, in order from strongest to weakest, is: Nd > Ni > Ba > K. The calculated strong binding of Ni and Nd to DOM is consistent with their affinity to form strong coordinate linkages with DOM molecules (Stevenson, 1994). The Visual MINTEQ speciation calculations provide a reasonable estimation of metal–DOM speciation and compare favourably with other studies. Rare earth element–DOM speciation modeling of peat groundwaters from the Great Dismal Swamp, Virginia conducted by Johannesson et al. (2004) indicated that Nd–DOM species accounted for between 60% and nearly 100% of the total metal concentration. They reported pH, ionic strength and DOC concentrations similar to values reported in the present study. Additionally, Unsworth et al. (2006) compared experimentally derived concentrations of Ni–DOM complexes with Visual MINTEQ calculated Ni–DOM concentrations for the same waters. Their results showed similar values for calculated and modeled Ni–DOM fractions, suggesting Visual MINTEQ accurately predicts metal–DOM complexation.

Metal–DOM complexation profiles along sampling transects indicate that concentrations of Ba and K are more sensitive to changes in the peat groundwater geochemistry compared with concentrations of Nd and Ni. Modeling calculations predict that the fraction of K bound to DOM is typically less than 50%, and only under the most ombrotrophic conditions do the total concentrations approach 100% DOM–bound (Fig. 8). The peat groundwater geochemistry at sites where smaller contributions of upwelling minerotrophic groundwater show a much greater decrease in calculationed Ba and K DOM complexes compared with Nd and Ni. This change in peat groundwater geochemistry likely resulted in the lower DOM binding affinities of Ba and K. Alkali metals only bind via electrostatic forces, whereas alkaline earth metals bind at specific sites. However, alkaline earth metals do not bind as strongly to DOM as transition metals due to the ion spherical symmetry and low polarizability of alkaline earth metals (Clymo, 1983; Stevenson, 1994; Tipping, 2002).

There are four factors that may limit the ability of metals to complex with DOM: (1) variability in pH; (2) type of DOM (i.e., fulvic or humic acid); (3) the ionic strength of peat groundwaters; and (4) variations in DOC concentrations. Research has previously shown that increases in pH result in a greater capacity for metals to bind to DOM (Lu and Allen, 2002; Pourret et al., 2007; Tipping, 2002). Higher pH values in waters typically result in less competition by H^+ ion activity for DOM binding sites. With less competition, a greater fraction of dissolved Ni and Nd can bind to DOM because they can fill more available binding sites. Conversely, under low pH conditions, elevated H^+ ion activity exerts stronger

competitive effects and commonly fills more of the available binding sites on organic molecules. Competition from H^+ effectively inhibits other dissolved metals from binding with DOM, resulting in greater concentrations of free ions in water. However, the study indicates that the calculated fraction of metal–DOM species decreases with increasing pH (Figs 5 and 8), suggesting that pH is not likely a limiting factor in metal complexation with DOM, particularly at sites of upwelling. It is possible that the poor association of pH with metal–DOM complexation is due to elevated carbonate alkalinity in minerotrophic peat groundwaters such as 300 m from the end of the Zulu transect, 307 m from the end of Golf, and at point-source locations along Yankee (Table 1).

Elevated carbonate alkalinity at these sites likely buffers the normally acidic peat groundwaters. The source of the high alkalinity could be from groundwater interactions with kimberlite, limestone or Tyrell Sea sediment, or some combination of these sources. Additionally, Tang and Johannesson (2010) showed that carbonate ions can outcompete fulvic acid for REEs, but not humic acids.

The most likely explanation for the decrease in metal–DOM complexation at sites with elevated upwelling minerotrophic groundwater is a combination of lower DOM concentrations coupled with increased ionic strength. This combination likely enhances competition effects, as there are more metal ions in the peat groundwaters competing for fewer DOM binding sites. The correlation between increases in ionic strength and decreases in the calculated fraction of Ni and Nd–DOM complexes is statistically significant ($r = -0.71$ and -0.94, respectively). The lower correlation coefficient for Ni compared with that for Nd might be attributed to the lower affinity of divalent Ni to bind to DOM. Elevated concentrations of alkaline earth metals such as Ca and Mg (major contributors to ionic strength) can induce strong competitive effects that inhibit metal binding to DOM (Cabaniss and Shuman, 1988a,b; Tipping, 2002). In the study, Ca and Mg concentrations are up to 25 times more elevated in minerotrophic peat groundwaters than in peat groundwaters with little to no detectable upwelling groundwater, and are 6–7 orders of magnitude greater than concentrations of Ni and Nd.

5.2. Controls on metal solubility

5.2.1. Metal binding and adsorption

The results of this study suggest that metal speciation is a key determining factor in kimberlite pathfinder metal solubility in peat groundwaters. The concomitant decrease in total Ni and Nd concentrations in peat groundwater and the decrease in the calculated fraction of these metals complexed with DOM (Figs. 5 and 8) suggest they may have been scavenged from solution due to their presence in greater proportions as free ions. Conversely, metals complexed with DOM are generally inhibited from participating in adsorption processes (Lofts and Tipping, 1998; Radovanovic and Koelmans, 1998; Sholkovitz and Copland, 1981) and, therefore, they tend to remain in solution. For example, elevated Ni and Nd concentrations along sampling transects occur at the east and west margins at Zulu and Golf, respectively, and at 350 m at Yankee (Fig. 8). With the exception of the Yankee sample site, these sites

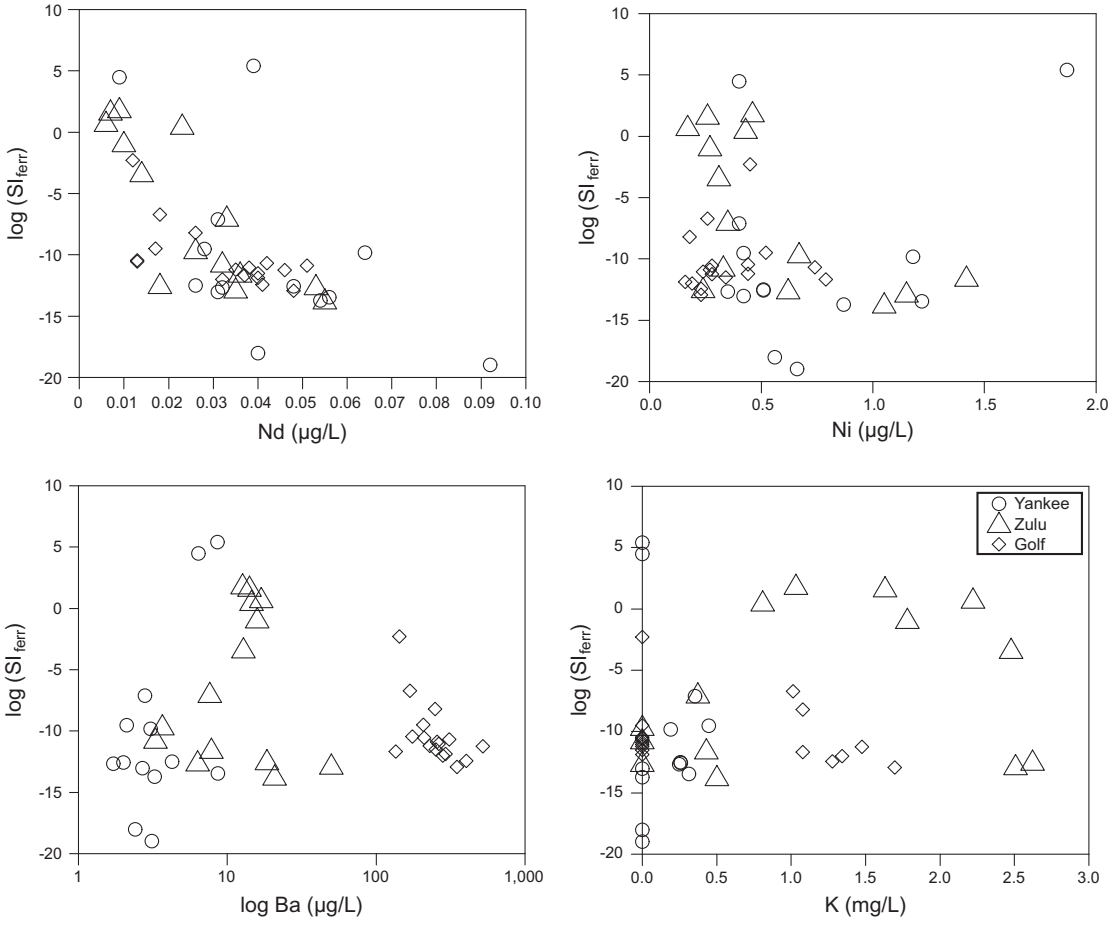

Fig. 12. Plots of Nd and Ni versus SI_{ferr} for peat groundwater samples from Yankee, Zulu and Golf ($n = 42$) indicate the highest concentrations of these metals are usually found where the SI_{ferr} is the lowest, likely due to their affinity to bind to ferrihydrite. Conversely, there is little correlation of SI_{ferr} with Ba and no correlation with K.

represent only small contributions from upwelling groundwaters and have high predicted fractions of Ni and Nd–DOM complexes. However, where upwelling of minerotrophic groundwater is greater, such as 400–700 m at Zulu, 400–700 m at Golf, and 443 and 489 m at Yankee, total Ni and Nd concentrations are commonly lower than local baseline peat groundwater values (Sader et al., 2011). The low Ni and Nd concentrations suggest that they have been scavenged from solution. Further evidence for metal scavenging is the elevated concentrations of Nd and Ni in peat digestion (Hattori and Hamilton, 2008), and these coincide with sites where total Ni and Nd concentrations and Ni and Nd fractions complexed with DOM are low (Fig. 8). It should be noted that metal–DOM complexes may adsorb to ferrihydrite (where present), and may also scavenge soluble metals. Davranche et al. (2005) found that REE–DOM complexes can adsorb onto the surfaces of MnO_2, thus resulting in REE–DOM–MnO_2 ternary complexes. However, in this study it is not possible to determine the extent to which this pathway may be active, as there are currently no models able to address the intricacies of the adsorption of these complexes.

The formation of ferrihydrite at sites of upwelling is likely critically important in scavenging metals where they dominantly exist as free ions. Peat groundwaters are close to or greater than saturation with respect to ferrihydrite at sites of high groundwater contributions (EC > 100 μS/cm), but well below saturation where conditions indicate little to no groundwater contribution (EC > 100 μS/cm) (Fig. 10). Overall, the $\log SI_{ferr}$ values are lower along the Golf sampling transect, and this is likely a function of the shallow sampling depth (0.4 mbgs) and lower pH. Additionally, the $\log SI_{ferr}$ correlates moderately well ($r = 0.72$) with peat Fe content from total peat digestion reported by Hattori and Hamilton (2008), and supports the validity of $\log SI_{ferr}$ calculations.

Decreases in total Ni and Nd and decreases in the calculated fraction of these metals complexed with DOM, coupled with increases in ferrihydrite suggest metals may be adsorbing on ferrihydrite where they exist as free ions. A plot of Nd versus $\log SI_{ferr}$ (Fig. 12) defines a trend of decreasing concentration with increasing $\log SI_{ferr}$. Nickel concentrations also decrease with increasing $\log SI_{ferr}$, however, the trend is not as defined as Nd, and this is likely because Nd is trivalent and has a stronger affinity to adsorb on Fe-oxyhydroxides (Stevenson, 1994). Conversely, alkali and alkaline earth metals (K and Ba) do not generally have a high affinity to adsorb on ferrihydrite (Cornell and Schwertmann, 2003; Kinniburgh et al., 1976), especially in the acidic pH peat groundwaters of this study. Laboratory tests conducted by Kinniburgh et al. (1976) indicated the pH must be greater than 8.1 for 50% of dissolved Ca and Mg to adsorb onto the surfaces of Fe gels. Based on that observation, they suggested that alkaline earth metals have a low selectivity for adsorption on Fe-oxyhydroxides. Likewise, little association exists between peat groundwater Ba concentrations and $\log SI_{ferr}$ in this study (Fig. 12).

The Visual MINTEQ calculated predictions of metal adsorption on ferrihydrite surfaces along the Zulu and Golf sampling transects support the analytical results. Calculations predict Ni and Nd are increasingly scavenged onto ferrihydrite surfaces at sites with greater upwelling groundwater contributions, and reveal that up to 90% and 95% of soluble Ni and Nd, respectively, may adsorb onto ferrihydrite surfaces (Fig. 11). Additionally, sample sites with high predicted adsorption (up to 95%) represent the lowest fractions (ca. 20%) of soluble Ni and Nd complexed with DOM. Calculations of metal–DOM speciation and metal adsorption to ferrihydrite surfaces (Fig. 8 and 11) suggest decreases in Ni and Nd complexation coupled with an inversely proportional increase in Ni and Nd bound to ferrihydrite is due to the increased availability of free metal ions. Conversely, the calculations predict that Ba and K do not adsorb strongly due to their lack of adsorption affinity for ferrihydrite. The results and modeling of metal adsorption on ferrihydrite surfaces in this study compares favourably with sequential leach results of sphagnum peat from a peat bog in Estonia (Syrovetnik et al., 2007). These authors concluded that a significant fraction of the transition metals Pb, Zn and Mn had adsorbed to Fe-oxyhydroxides, whereas adsorption of alkaline earth metals was negligible.

Adsorption of metals onto insoluble humic substances may be partly responsible for scavenging metals where groundwaters are upwelling. Metals typically have a strong affinity to adsorb onto insoluble organic matter. The cation exchange capacity of sphagnum peat ranges from 0.6 to 2 meq/g at pH 7 and peat can retain high concentrations of metals (Hill and Siegel, 1991; Sikora and Keeney, 1983). However, it is suggested that Ni and Nd are more likely to adsorb onto ferrihydrite rather than insoluble organics. Alkali and alkaline earth metals are highly effective competitors for insoluble organic adsorption sites and will invariably compete strongly with Ni and Nd for such sites. This competition is likely strongest at sites of upwelling where alkaline earth concentrations are up to 25 times higher than ombrotrophic peat groundwaters. However, these metals will not compete strongly for ferrihydrite adsorption sites.

It is also possible that all insoluble organic adsorption sites have been filled where groundwater upwelling is strong. Hill and Siegel (1991) noted that insoluble organic cation exchange sites are full in spring-fen condition sphagnum peat bogs. In the present study, the elevated Ca and Mg at sites of strong upwelling may indicate a similar scenario, where all insoluble organic adsorption sites are filled. The contribution rate of alkali and alkaline earth metal inputs to peat groundwaters at sites of strong groundwater upwelling may exceed the rate of peat humification and production of insoluble organic substances. The ca. 3 m layer of peat in the study area accumulated over approximately 5 ka. If these adsorption sites were full, transition metals would be more likely to adsorb to ferrihydrite because of the lack of insoluble organic adsorption sites.

5.2.2. Secondary mineral precipitation

Carbonate and sulfide mineral precipitation are capable of scavenging metals from solution in many environments. However, in this study it is reasonable to exclude these processes as possible scavengers of dissolved metals. The $\log SI_{calcite}$ for all peat groundwater samples is <0 and, therefore, calcite is not favoured to form. It should, however, be noted that loss on ignition and ammonium acetate leach (pH 5) analyses of Attawapiskat peat (Brauneder, 2007; Hattori and Hamilton, 2008) provide evidence of carbonate precipitation in peat samples collected at 0.6 mbgs along sampling transects nearly identical to those in this study. However, peat groundwater samples in this study were collected at 1.1 mbgs at Yankee and Zulu and 0.4 mbgs at Golf and likely represent different geochemical zones within the peat. Peat groundwater geochemistry such as Ca concentration, pH and alkalinity can vary substantially over small changes in depth (Clymo, 1983), which will impact calcite saturation.

Sulfide minerals are not thought to appreciably scavenge soluble metals in this study. Both sulfate and total S concentrations are low in the peat groundwaters and no correlation exists between concentrations of sulfate and S, and sites of upwelling groundwaters (Table 1). Additionally Hattori and Hamilton (2008) noted that total S content of peat is below 0.1% at all of their sample sites.

6. Summary and implications for mineral exploration

This study highlights the importance of metal–DOM complexation in geochemical exploration and the effect those complexes can have on the solubility of metals in water saturated environments

such as wetlands. The saturated nature of wetlands and the high DOC concentrations in peat groundwaters adds another level of complexity with respect to surficial geochemical exploration, as dissolved metals are not only governed by precipitation and adsorption processes onto solid media, but by metal–DOM complexes that can prevent metal adsorption and increase solubility. For example, it has been shown here that Nd concentrations are elevated at sample sites with minor contributions of upwelling groundwaters at or near kimberlite margins at Zulu and Golf. At these sites the modeling calculations indicate nearly 100% of the transition metals form DOM complexes. Conversely, where the modeling calculations indicate low Nd and Ni–DOM complexes, such as at site 07-Y-12 at Yankee, and at the east ends of the Zulu and Golf sampling transects, the metal concentrations in peat groundwater are less than baseline values. Modeling calculations predict that the low metal concentrations at these sites are due to a greater ability for Ni and Nd (which exist as free ions) to adsorb on ferrihydrite surfaces.

In contrast to the high DOM, water saturated peat bog environment of this study, soluble metals in groundwaters employed in mineral exploration typically do not consider DOM concentrations (Leybourne and Cameron, 2010; Sader et al., 2007). Dissolved organic matter concentrations are low in most natural groundwaters (Freeze and Cherry, 1979) and, therefore, they are not dominant in the control of soluble metal behaviour. The findings also contrast with the findings of geochemical studies of soil collected above the water table for mineral exploration, where adsorption onto solid phase organics and ferrihydrite are more important aspects for detecting pathfinder metals.

This study has implications for surficial geochemical exploration for mineral deposits, as metal speciation and metal adsorption affinities are important aspects that must be considered when establishing effective sampling and analytical methodologies. It also has implications for the spatial distribution of metals in soils, peat and groundwaters where high DOM conditions exist. For wetland environments, the results indicate that the most effective means to accurately detect kimberlite pathfinder metals is to collect samples from both peat and peat groundwater samples along sampling transects. The collection of both media likely provides a more accurate delineation of metals associated with a buried kimberlite. If the peat groundwaters are dominantly ombrotrophic with only minor contributions from kimberlite groundwaters, metals are more likely to remain highly soluble as metal–DOM complexes. A geochemical exploration sampling program that only focuses on peat may overlook important geochemical responses, as the formation of metal–DOM complexes may inhibit metal adsorption or incorporation into secondary mineral precipitates. Conversely, if only peat groundwaters are collected, a kimberlite geochemical response may also be overlooked where kimberlite pathfinder metals are migrating upwards into peat groundwaters that have the potential to scavenge dissolved metals (more minerotrophic conditions). The results suggest scavenging of metals, which exist as free ions by ferrihydrite or insoluble organic matter, is the most likely pathway.

Acknowledgements

We thank DeBeers Canada for providing financial and logistical support for the project. Julie Kong, Ed Francisco and Brad Wood were particularly helpful. Financial support was also provided by a NSERC Discovery grant and a NSERC Collaborative Research grant to Keiko Hattori. Jamil Sader received financial support from an Ontario Graduate Scholarship and a student research grant from the Society of Economic Geologists. Fieldwork was assisted by Katherine Mellor. We thank M. Beth McClenaghan and Jan Peter (Geological Survey of Canada), Matt Leybourne (GNS New Zealand), and Karen Johannesson (Tulane University) for insightful comments on an earlier version of the manuscript. Journal reviewers Clemens Reimann and Olivier Pourret, and Editor Ron Fuge provided thorough and insightful reviews that greatly benefited this paper.

References

Armstrong, J.P., Wilson, M., Barnett, R.L., Nowicki, T., Kjarsgaard, B.A., 2004. Mineralogy of primary carbonate-bearing hypabyssal kimberlite, Lac de Gras, Slave Province, Northwest Territories, Canada. Lithos 76, 415–433.

Astrom, M.E., Nystrand, M., Gustafsson, J.P., Osterholm, P., Nordmyr, L., Reynolds, J.K., Peltola, P., 2010. Lanthanoid behaviour in an acidic landscape. Geochim. Cosmochim. Acta 74, 829–845.

Bell, R.A., Ogden, N., Kramer, J.R., 2002. The biotic ligand model and a cellular approach to class B metal aquatic toxicity. Comp. Biochem. Physiol. C: Pharmacol. Toxicol. 133, 175–188.

Bellefleur, G., Matthews, L., Roberts, B., McMonnies, B., Salisbury, M., Snyder, D., Perron, G., McGaughey, J., 2005. Downhole seismic imaging of the Victor Kimberlite, James Bay Lowlands, Ontario; a feasibility study. Geol. Surv. Can. Open File Report 2005-C1.

Benedetti, M.F., Van Riemsdijk, W.H., Koopal, L.K., Kinniburgh, D.G., Gooddy, D.C., Milne, C.J., 1996. Metal ion binding by natural organic matter: from the model to the field. Geochim. Cosmochim. Acta 60, 2503–2513.

Boelter, D.H., Verry, E.S., 1977. Peatland and water in the northern Lake States. General Technical Report NC-31, U.S. Department of Agriculture, Forest Service, St. Paul, MN.

Brauneder, K., 2007. Characterization of peatland waters overlying concealed kimberlites in the Attawapiskat region, northern Ontario. B.Sc. Hon. Thesis, Univ. Ottawa.

Bruland, K.W., Donat, J.R., Hutchins, D.A., 1991. Interactive influences of bioactive trace metals on biological production in oceanic waters. Limnol. Oceanog. 36, 1555–1577.

Bryan, S.E., Tipping, E., Hamilton-Taylor, J., 2002. Comparison of measured and modelled copper binding by natural organic matter in freshwaters. Comp. Biochem. Physiol. C: Toxicol. Pharmacol. 133, 37–49.

Cabaniss, S.E., Shuman, M.S., 1988a. Copper binding by dissolved organic matter: I. Suwannee River fulvic acid equilibria. Geochim. Cosmochim. Acta 52, 185–193.

Cabaniss, S.E., Shuman, M.S., 1988b. Copper binding by dissolved organic matter: II. Variation in type and source of organic matter. Geochim. Cosmochim. Acta 52, 195–200.

Cameron, E.M., Hamilton, S.M., Leybourne, M.I., Hall, G.E.M., McClenaghan, M.B., 2004. Finding deeply buried deposits using geochemistry. Geochem. Explor. Environ. Anal. 4, 7–32.

Clymo, R.S., 1983. Peat. In: Gore, A.J.P. (Ed.), Mires: Swamp, Bog, Fen and Moor. Elsevier Scientific, Amsterdam, pp. 159–224.

Cornell, R.M., Schwertmann, U., 1979. Influence of organic anions on the crystallization of ferrihydrite. Clays Clay Min. 27, 402–410.

Cornell, R.M., Schwertmann, U., 2003. The Iron Oxides; Structure, Properties, Reactions, Occurrence and Uses. Wiley-VCH, Weinheim.

Cowell, D.W., 1983. Karst hydrogeology within a subarctic peatland: Attawapiskat River, Hudson Bay lowland, Canada. J. Hydrol. 61, 169–175.

Davranche, M., Pourret, O., Gruau, G., Dia, A., Le Coz-Bouhnik, M., 2005. Adsorption of REE(III)-humate complexes onto MnO2: experimental evidence for cerium anomaly and lanthanide tetrad effect suppression. Geochim. Cosmochim. Acta 69, 4825–4835.

Dwane, G.C., Tipping, E., 1998. Testing a humic speciation model by titration of copper-amended natural waters. Environ. Int. 24, 609–616.

Dzombak, D.A., Morel, F.M.M., 1990. Surface Complexation Modeling; Hydrous Ferric Oxide. John Wiley & Sons, New York.

Filzmoser, P., Hron, K., Reimann, C., 2010. The bivariate statistical analysis of environmental (compositional) data. Sci. Total Environ. 408, 4230–4238.

Freeze, R.A., Cherry, J.A., 1979. Groundwater. Prentice-Hall, Inc., Englewood Cliffs, N.J.

Gustafsson, J.P., 2010. Visual MINTEQ 3.0 For Windows XP/7.

Hattori, K.H., Hamilton, S., 2008. Geochemistry of peat over kimberlites in the Attawapiskat area, James Bay Lowlands, northern Canada. Appl. Geochem. 23, 3767–3782.

Hattori, K.H., Hamilton, S.M., Kong, J., Gravel, J., 2009. Soil geochemical survey over concealed kimberlites in the Attawapiskat area in northern Canada. Geochem. Explor. Environ. Anal. 9, 139–150.

Hill, B.M., Siegel, D.I., 1991. Groundwater flow and the metal content of peat. J. Hydrol. 123, 211–224.

Hoag, R.S., Price, J.S., 1995. A field-scale, natural gradient solute transport experiment in peat at a Newfoundland blanket bog. J. Hydrol. 172, 171–184.

Hoch, A.R., Reddy, M.M., Aiken, G.R., 2000. Calcite crystal growth inhibition by humic substances with emphasis on hydrophobic acids from the Florida Everglades. Geochim. Cosmochim. Acta 64, 61–72.

Ingram, H.A.P., 1983. Hydrogeology. In: Gore, A.J.P. (Ed.), Mires: Swamp, Bog. Fen and Moor. Elsevier Scientific, Amsterdam, pp. 67–158.

Johannesson, K.H., Tang, J., Daniels, J.M., Bounds, W.J., Burdige, D.J., 2004. Rare earth element concentrations and speciation in organic-rich blackwaters of the Great Dismal Swamp, Virginia, USA. Chem. Geol. 209, 271–294.

Khai, N.M., Öborn, I., Hillier, S., Gustafsson, J.P., 2008. Modeling of metal binding in tropical fluvisols and acrisols treated with biosolids and wastewater. Chemosphere 70, 1338–1346.

Kinniburgh, D.G., Jackson, M.L., Syers, J.K., 1976. Adsorption of alkaline earth, transition, and heavy metal cations by hydrous oxide gels of iron and aluminum. Soil Sci. Soc. Am. J. 40, 796–799.

Kinniburgh, D.G., van Riemsdijk, W.H., Koopal, L.K., Borkovec, M., Benedetti, M.F., Avena, M.J., 1999. Ion binding to natural organic matter: competition, heterogeneity, stoichiometry and thermodynamic consistency. Colloids Surf A: Physicochem. Eng. Aspects 151, 147–166.

Kong, J.M., Boucher, D.R., Scott Smith, B.H., 1999. Exploration and geology of the Attawapiskat Kimberlites, James Bay Lowland, northern Ontario, Canada. In: Gurney, J.J., Gurney, J.L., Pascoe, M.D., Richardson, S.H. (Eds.), The J Dawson Volume. Proc. Int. Kimberlite Conf., Cape Town, pp. 452–467.

Koopal, L.K., van Riemsdijk, W.H., de Wit, J.C.M., Benedetti, M.F., 1994. Analytical Isotherm Equations for Multicomponent Adsorption to Heterogeneous Surfaces. J. Colloid Interf. Sci. 166, 51–60.

Leybourne, M.I., Cameron, E.M., 2010. Ground water in geochemical exploration. Geochem. Explor. Environ. Anal. 10, 99–118.

Lofts, S., Tipping, E., 1998. An assemblage model for cation binding by natural particulate matter. Geochim. Cosmochim. Acta 62, 2609–2625.

Lu, Y., Allen, H.E., 2002. Characterization of copper complexation with natural dissolved organic matter (DOM)–link to acidic moieties of DOM and competition by Ca and Mg. Water Res. 36, 5083–5101.

Mann, A.W., Birrell, R.D., Mann, A.T., Humphreys, D.B., Perdrix, J.L., 1998. Application of the mobile metal ion technique to routine geochemical exploration. J. Geochem. Explor. 61, 87–102.

McClenaghan, M.B., Hamilton, S.M., Hall, G.E.M., Burt, A.K., Kjarsgaard, B.A., 2006. Selective Leach Geochemistry of Soils Overlying the 95-2, B30, and A4 Kimberlites, Northeastern Ontario. Geol. Surv. Can. – Open-File Rep. 5069: 31.

Milne, C.J., Kinniburgh, D.G., van Riemsdijk, W.H., Tipping, E., 2003. Generic NICA – donnan model parameters for metal-ion binding by humic substances. Environ. Sci. Technol. 37, 958–971.

Norris, A.W., 1993. Hudson platform: introduction. In: Stott, D.F., Aitken, J.D. (Eds.), Sedimentary Cover of the Craton in Canada. Geol. Surv. Canada, Ottawa.

Paquin, P.R., Gorsuch, J.W., Apte, S., Batley, G.E., Bowles, K.C., Campbell, P.G.C., Delos, C.G., Di Toro, D.M., Dwyer, R.L., Galvez, F., Gensemer, R.W., Goss, G.G., Hogstrand, C., Janssen, C.R., McGeer, J.C., Naddy, R.B., Playle, R.C., Santore, R.C., Schneider, U., Stubblefield, W.A., Wood, C.M., Wu, K.B., 2002. The biotic ligand model: a historical overview. Comp. Biochem. Physiol. C: Pharmacol. Toxicol. 133, 3–35.

Perdue, E.M., Ritchie, J.D., 2005. Dissolved organic matter in freshwaters. In: Drever, J.I. (Ed.), Surface and Ground Water, Weathering, and Soils, vol 8. In: Holland, H.D., Turekian, K.K. (Exec. Eds.), Treatise on Geochemistry. Elsevier Ltd., Oxford, UK, 273–318.

Pourret, O., Davranche, M., Gruau, G., Dia, A., 2007. Rare earth elements complexation with humic acid. Chem. Geol. 243, 1–2.

Radovanovic, H., Koelmans, A.A., 1998. Prediction of in situ trace metal distribution coefficients for suspended solids in natural waters. Environ. Sci. Technol. 32, 753–759.

Ravichandran, M., Aiken, G.R., Ryan, J.N., Reddy, M.M., 1999. Inhibition of precipitation and aggregation of metacinnabar (mercuric sulfide) by dissolved organic matter isolated from the Florida everglades. Environ. Sci. Technol. 33, 1418–1423.

Ronnback, P., Astrom, M., Gustafsson, J.-P., 2008. Comparison of the behaviour of rare earth elements in surface waters, overburden groundwaters and bedrock groundwaters in two granitoidic settings, Eastern Sweden. Appl. Geochem. 23, 1862–1880.

Sader, J.A., Anderson, H.S.I., Fenstermacher, R.F., Hattori, K.H., 2009. Imaging a buried diamondiferous kimberlite using conventional geochemistry and amplified geochemical imaging technology. In: Lentz, D.R., Thorne, K.G., Beal, K. (Eds.), 24th Internat. Symp. Applied Geochemistry. Association of Applied Geochemists, Fredericton, NB, Canada, 561–564.

Sader, J.A., Hattori, K.H., Kong, J.M., Hamilton, S.M., 2011. Geochemical responses in peat groundwater over Attawapiskat kimberlites, James Bay Lowlands, Canada and their application to diamond exploration. Geochem. Explor. Environ. Anal. in press.

Sader, J.A., Leybourne, M.I., McClenaghan, M.B., Hamilton, S.M., 2007. Low-temperature serpentinization processes and kimberlite ground water signatures in the Kirkland Lake and Lake Timiskiming kimberlite fields, Ontario, Canada; implications for diamond exploration. Geochem. Explor. Environ. Anal. 7, 3–21.

Sage, R.P., 2000. Kimberlites of the Attawapiskat Area, James Bay Lowlands, Northern Ontario. Ontario Geol. Surv. Open File Report 6019.

Shilts, W.W., 1986. Glaciation of the Hudson Bay Region. In: Martini, I.P. (Ed.), Canadian Inland Seas. Elsevier Science, Amsterdam, pp. 55–78.

Sholkovitz, E.R., Copland, D., 1981. The coagulation, solubility and adsorption properties of Fe, Mn, Cu, Ni, Cd, Co and humic acids in a river water. Geochim. Cosmochim. Acta 45, 181–189.

Sikora, L.J., Keeney, D.R., 1983. Further Aspects of Soil Chemistry Under Anaerobic Conditions. In: Gore, A.J.P. (Ed.), Mires: Swamp, Bog, Fen and Moor. Elsevier Scientific, Amsterdam, pp. 247–256.

Sonke, J.E., Salters, V.J.M., 2004. Determination of neodymium-fulvic acid binding constants by capillary electrophoresis inductively coupled plasma mass spectrometry (CE-ICP-MS). J. Anal. Atom. Spectrom. 19, 235–240.

Stevenson, F.J., 1994. Humus Chemsitry: Genesis, Composition, Reactions. John Wiley & Sons, Inc., New York.

Syrovetnik, K., Malmstrom, M.E., Neretnieks, I., 2007. Accumulation of heavy metals in the Oostriku peat bog, Estonia: determination of binding processes by means of sequential leaching. Environ. Pollut. 147, 291–300.

Tang, J., Johannesson, K.H., 2005. Adsorption of rare earth elements onto Carrizo sand: experimental investigations and modeling with surface complexation. Geochim. Cosmochim. Acta 69, 5247–5261.

Tang, J., Johannesson, K.H., 2010. Ligand extraction of rare earth elements from aquifer sediments: Implications for rare earth element complexation with organic matter in natural waters. Geochim. Cosmochim. Acta. 74, 6690–6705.

Thurman, E.M., 1985. Organic Geochemistry of Natural Waters. Martinus Nijhoff/Dr. W. Junk Publishers, Dordrecht, NL.

Tipping, E., 2002. Cation Binding by Humic Substances. Cambridge Environmental Chemistry Series, vol. 12. Cambridge University Press.

Unsworth, E.R., Warnken, K.W., Zhang, H., Davison, W., Black, F., Buffle, J., Cao, J., Cleven, R., Galceran, J., Gunkel, P., Kalis, E., Kistler, D., van Leeuwen, H.P., Martin, M., Noel, S., Nur, Y., Odzak, N., Puy, J., van Riemsdijk, W., Sigg, L., Temminghoff, E., Tercier-Waeber, M.-L., Toepperwien, S., Town, R.M., Weng, L., Xue, H., 2006. Model predictions of metal speciation in freshwaters compared to measurements by in situ techniques. Environ. Sci. Technol. 40, 1942–1949.

van Straaten, B.I., Kopylova, M.G., Russell, J.K., Webb, K.J., Smith, B.H.S., 2009. Stratigraphy of the intra-crater volcaniclastic deposits of the Victor Northwest kimberlite, northern Ontario, Canada. Lithos 112 (Supp. 1), 488–500.

Webb, K.J., Scott Smith, B.H., Paul, J.L., Hetman, C.M., 2004. Geology of the Victor Kimberlite, Attawapiskat, northern Ontario, Canada; cross-cutting and nested craters. Lithos 76, 29–50.